Annals of Physics **275**, 151–189 (1999)
Article ID aphy.1999.5932, available online at http://www.idealibrary.com on IDEAL®

The Inverse Scattering Problem for Chaotic Hamiltonian Systems

C. Jung

Centro Internacional de Ciencias, Cuernavaca, Mexico; and Instituto de Matematicas, Unidad Cuernavaca, University of Mexico (UNAM), 62251 Cuernavaca, Mexico

C. Lipp

Centro Internacional de Ciencas, Cuernavaca, Mexico; and Institut für theoretische Physik, Universität Basel, Klingelbergstrasse 82, 4056 Basel, Switzerland

and

T. H. Seligman

Centro Internacional de Ciencias, Cuernavaca, Mexico; and Instituto de Matematicas, Unidad Cuernavaca, University of Mexico (UNAM), 62251 Cuernavaca, Mexico

Received December 11, 1997; revised January 13, 1999

We propose an analysis of the inverse scattering problem for chaotic Hamiltonian systems. Our main goal will be the reconstruction of the structure of the chaotic saddle from asymptotic data. We will also address the question how to obtain thermodynamic measures and a partition from these data. An essential step in achieving this is the reconstruction of the hierarchical order of the fractal structure of singularities in scattering functions solely from knowledge of asymptotic data. This provides a branching tree which coincides with the branching tree derived from the hyperbolic component of the horseshoe in the Poincaré map taken in the interaction region. We achieve our goal explicitly for two types of systems governed by an external or an internal clock, respectively. Once we have achieved this goal, a discrete arbitrariness remains for the reconstruction of the horseshoe. Here symmetry considerations can help. We discuss the implications for the inverse scattering problem of the effects of finite resolution and the possible use of nonhyperbolic effects. The connection between the formal development parameter of the horseshoe and the topological entropy proves helpful in the systems discussed.

0003-4916/99 $30.00

1. INTRODUCTION

The inverse scattering problem is extensively studied in wave dynamics for almost any kind of waves, such as electrodynamical, sound, elastic, and quantum mechanical waves. The applications are numerous and include very important and practical ones such as radar, sonar, ultrasonography, tomography, geological exploration, and remote perception as well as more abstract questions such as the understanding of processes in the interaction region from nuclear, atomic, or molecular scattering data.

Yet any of these wave processes has an associated ray problem that—at least for scalar fields—is much simpler and corresponds to a short wave approximation. The purpose of the present paper is to study the inverse scattering problem for precisely such ray problems. This implies essentially that we shall look at the inverse scattering problem for classical mechanics. Ray acoustics and ray optics in the absence of polarization effects do not differ significantly.

The practical importance of this question is certainly much more limited for ray problems than for wave problems. Nevertheless we believe that the question is of interest. The mathematical problem in itself is challenging, and in the presence of experimental error it may be essential to know how much we can learn from a given type of experiment, namely the scattering experiment. Furthermore we may well be interested in knowing what behavior of the scattering functions may be typical for what dynamics in the interaction region. The possible implication for wave dynamics resides in semi-classical approaches. The word "semi-classical" stems from the relation between quantum and classical dynamics but carries over to that between ray and wave dynamics in other fields.

The inverse scattering problem for integrable systems usually implies reconstructing, from scattering data, the potential or the Hamiltonian under severely restrictive conditions for their form. Typical examples are rotationally invariant and monotonic potentials where closed solutions are available (see [1] and Section 5.9 in [2]). In chaotic systems such an attempt seems hopeless and what is more, uninteresting. We are mainly interested in a structural understanding of the dynamics. For a system of chaotic scattering this means in particular some knowledge of the structure of the chaotic invariant set, the so-called chaotic saddle, and of its partition and its thermodynamic quantities. At the moment nobody knows how to obtain them directly from the functional form of the Hamiltonian or the potential. In this sense the construction of some analytic fit for the Hamiltonian or for the potential is unnecessary. As an alternative we propose a direct attempt to reconstruct the topological structure as well as some statistical properties of the chaotic saddle from asymptotic data. This includes the attempt to obtain a symbolic dynamic.

These properties are in turn essentially given by the periodic orbit structure and their homoclinic and heteroclinic connections. For systems of many degrees of freedom this structure is complicated and little explored. We shall thus at this stage restrict our attention to the two simplest cases: time-dependent systems with one degree of freedom and time independent systems with two degrees of freedom.

For the integrable case the inverse problem usually refers to cross sections, which implies some integration over initial conditions. The matter of obtaining scattering functions from them is a complication we shall omit by assuming that scattering functions are directly available as asymptotic data.

Furthermore the inverse scattering problem typically appears in two presentations: the physical one, where finite exactitude in the measurement of the scattering functions is considered; and the more mathematical one, where we assume that we have arbitrarily exact information about these functions.

In the latter case we first must identify the hierarchical structure of the singularities of the scattering functions. This leads to a branching tree and we can then ask whether this tree is sufficient to characterize the topology of the chaotic saddle.

For integrable systems the errors in the measurement of the scattering functions usually have two consequences: First and quite logically they imply errors in the parameters of the Hamiltonian or potential we extract. This is to be expected and is not serious. On the other hand discrete ambiguities are usually found and sometimes infinite families of such. Some extra knowledge about the system is typically invoked, to select the, it is hoped correct but actually often wrong solution. In our analysis of chaotic systems we shall find much the same picture.

An obvious first step in the direction we wish to go was given in [3]. There we discussed the question, in what circumstances are we able to distinguish systems belonging to one of the three classes: systems that have integrable scattering map, systems with integrable Hamiltonian flow but chaotic scattering map and, finally systems having topological chaos in the flow? We will assume these results and concentrate on the last case.

We take advantage of the fact that numerical calculations can yield exact results about the topology of a chaotic saddle. This is due to the fact that the formal development parameter of a horseshoe remains constant while the physical parameter covers a finite interval. But the topology is at least partially determined by this formal parameter. We shall be able to give a positive answer to our question for periodically time dependent one-dimensional systems as well as for certain time-independent systems that carry, in a sense to be explained, their own built-in clocks. For more general systems we can only point out the difficulties and give some hints about the direction in which future work may proceed.

Our program and general line of argumentation will be as follows: First we introduce a formal parameter which gives approximately the development stages of horseshoes. The formal parameter approximates this development insofar as it gives the universal aspects and ignores the individual details of the special realization under consideration. In the following section we explain the scattering functions and their fractal set of singularities, which will be the input data for the reconstruction of the chaotic saddle from asymptotic data. The main ingredient is the hierarchical structure of intervals of continuity. We show that thermodynamical measures of chaos can be obtained if this hierarchical structure is known. In Section 4 we show for two classes of scattering systems how to find the hierarchical level

of each interval of continuity without resorting to observations in the interaction region. This provides the branching tree of the unstable component of the chaotic saddle. In the next section we point out the fact that unfortunately the branching tree does not yet determine the horseshoe. There remains a discrete arbitrariness concerning the basic type of horseshoe or the number of elementary fixed points involved. Sometimes this discrete uncertainty can be resolved by symmetry arguments. Section 6 discusses why the search and the observation of nonhyperbolicities and individual properties of the saddle are in general of no help in classifying the horseshoe from asymptotic measurements. In addition we discuss the influence of measurements with finite resolution.

2. CLASSIFICATION OF HORSESHOES

It is the goal of this paper to extract from asymptotic data information about the chaotic invariant set, represented by a horseshoe construction in an appropriate Poincaré section. Therefore we start by a description of our approximate classification of horseshoe structures. In particular we introduce a formal parameter, which is one of the quantities we want to find.

The Smale horseshoe construction is done by stretching a so-called fundamental rectangle R with the four corner points F, A, B, C and folding it back onto the original rectangle [4, 5]. Figure 1 shows this construction schematically for a binary horseshoe with two elementary fixed points. The boundaries of R are given by segments of the invariant manifolds of the outer fixed point F which are the lines plotted in this figure. By folding the fundamental rectangle two or more times one can construct horseshoes with larger numbers of elementary fixed points.

In chaotic systems we always have homoclinic and/or heteroclinic intersections of invariant manifolds. As Smale has shown [4], this is always connected with a horseshoe construction. Hereby a system with N elementary fixed points corresponds to a horseshoe with the same number of fixed points. However, it does not necessarily have to be a complete horseshoe. In principle one can obtain the horseshoe structure by plotting the invariant manifolds of any unstable periodic point.

It is advisable to use the manifolds of those fixed points which lie on the corners of R. Then the boundaries of R as well as the boundaries of all gaps which are cut into R by forming the intersection between R and its images and preimages are given by these manifolds. These gaps play an important role in the horseshoe structure since they are regions within R which are not needed to cover the invariant set. In particular no higher level tendrils of the invariant manifolds will ever enter such gaps. In each iteration step one further tendril of the manifolds is added and one further level of hierarchy of these gaps is displayed. Therefore we see clearly the construction scheme of the horseshoe by going from one level to the next by doing the next iteration. It is in analogy to the hierarchical construction of a Cantor set by giving level by level the endpoints of cutout intervals.

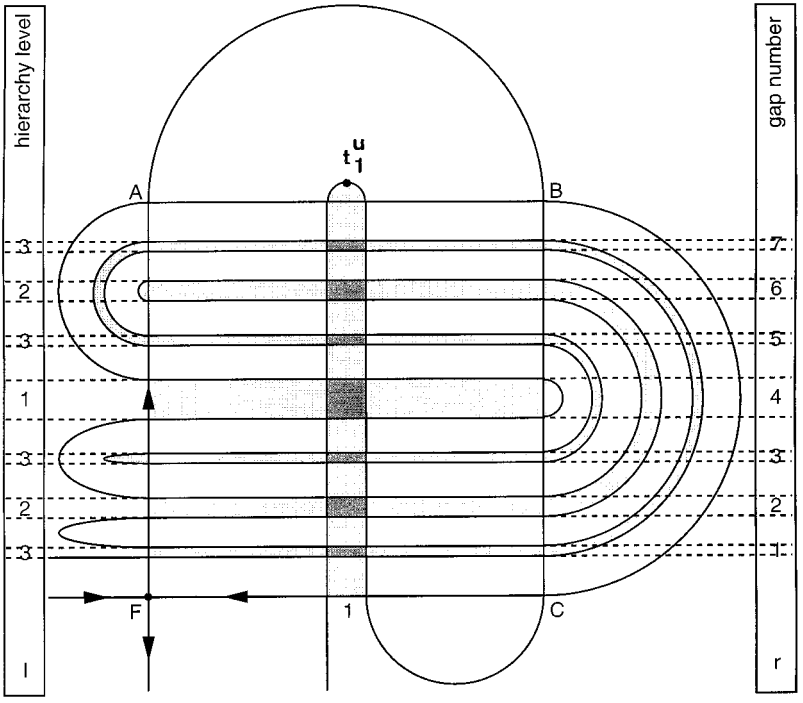

FIG. 1. Schematic plot of a complete binary horseshoe. The outer fixed point is labeled *F*. The fundamental rectangle *R* has the corners F, A, B, C. The stable manifold of *F* cuts gaps into *R*. Their hierarchical level is indicated by the numbers in the left column. The numbers in the right column count all gaps up to level 3 consecutively from bottom to top. The gaps cut into *R* by the tendrils of the invariant manifolds are shaded. The tendrils of the stable manifold of *F* are plotted up to level 3, the tendrils of the unstable manifold are plotted up to level 1. We indicate a complete binary horseshoe by the formal parameter value $\beta = 1$.

The tendrils of the invariant manifolds of periodic points lying in the interior of *R* do not have this favorable property of forming the boundaries of the gaps. Only infinite sequences of segments of their manifolds converge to the boundary lines. Therefore we need very high iterations of the tendrils of inner periodic points before we obtain a clear picture of the hierarchical construction of the horseshoe.

We introduce a formal parameter for the development stage of incomplete horseshoes along the ideas given in Refs. [6–8]. First, consider a complete binary horseshoe like the one shown in Fig. 1. The invariant manifolds of the fixed point *F* define the fundamental rectangle *R*. In the complete case the tip of the tendril of level 1 of the unstable manifold of *F*, which we denote by t_1^u, reaches the other side of the rectangle, thus splitting it into two parts. In the complete case the formal parameter is given by $\beta = 1$.

If we have an incomplete horseshoe, t_1^u does not reach the other side (it is located inside of *R*) and our formal parameter will be determined by the relative length of the tendril as compared to the complete case. If t_1^u ends in a gap produced by the

tendrils of the stable manifold of F we can introduce an approximate symbolic dynamics which holds up to a certain level of hierarchy. This dynamics holds for an interval of the physical development parameter and not only for a single point [6].

Therefore it is essential to label the gaps produced by the stable manifold in an appropriate way as indicated in Fig. 1. The gaps cut into R by the stable manifold of F are the shaded strips which intersect R horizontally. The left column gives the hierarchical level of the gaps that corresponds to the level of the tendril that creates the gap. The right column counts the gaps up to level 3 consecutively. If we consider only gaps of level $l \leqslant k$ and t_1^u ends in the rth gap then the formal parameter is given by

$$\beta = r2^{-k}. \tag{1}$$

An example of an incomplete horseshoe is shown schematically in Fig. 2: If we consider gaps up to level $k=2$ then t_1^u ends in the third gap from below, thus leading to the formal parameter $\beta = 3/4$. If we take gaps up to $k=3$ then it is the sixth gap, but the value for the formal parameter β remains the same.

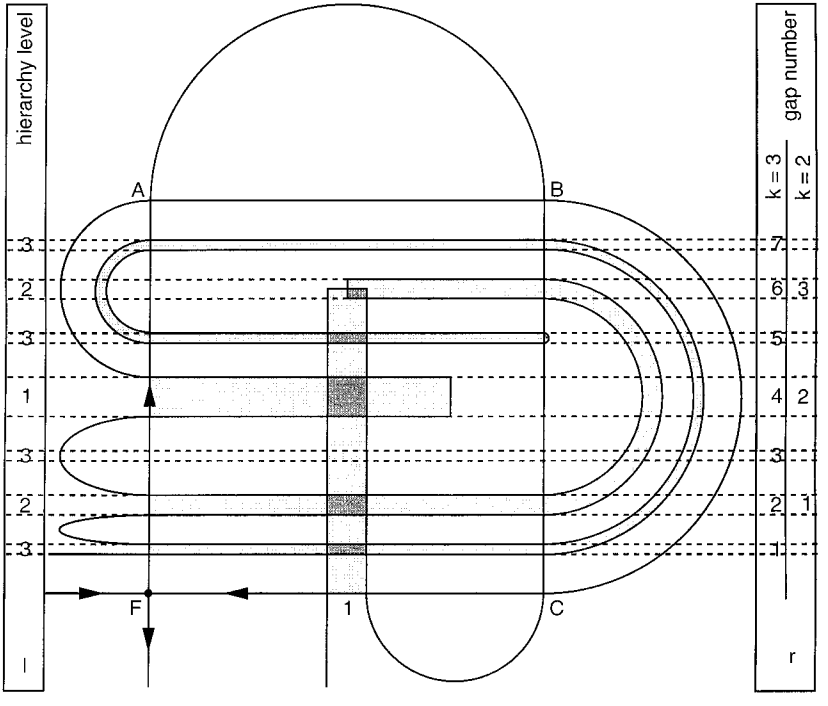

FIG. 2. Schematic plot of an incomplete binary horseshoe at formal parameter value $\beta = 3/4$. The labels are as in Fig. 1. In the column of the gap numbers we have shown these numbers for the case $k=2$ and also for the case $k=3$.

For horseshoes with three elementary fixed points things are a little different. Let us consider a ternary horseshoe with two fixed points F_1 and F_2 at opposite sides of the fundamental rectangle R. Here the boundaries of R are given by the manifolds, of F_1 and F_2. Therefore we have two tendrils of unstable manifolds, which gives us two formal development parameters. For ternary symmetric horseshoes these two outer fixed points as well as their manifolds are equivalent and mirror images of each other, so only one formal parameter is needed. Let us consider the ternary symmetric horseshoe more closely because we will use it frequently for demonstration purposes. The value of its formal parameter, which we will call γ, can be determined in analogy to the binary case by counting gaps, and the formula is given by

$$\gamma = r3^{-k}. \tag{2}$$

In the complete case shown in Fig. 3, t_1^u ends outside the fundamental rectangle, or in the ninth gap of order $l \leqslant 2$, which gives us the formal parameter $\gamma = 1$. Plotted

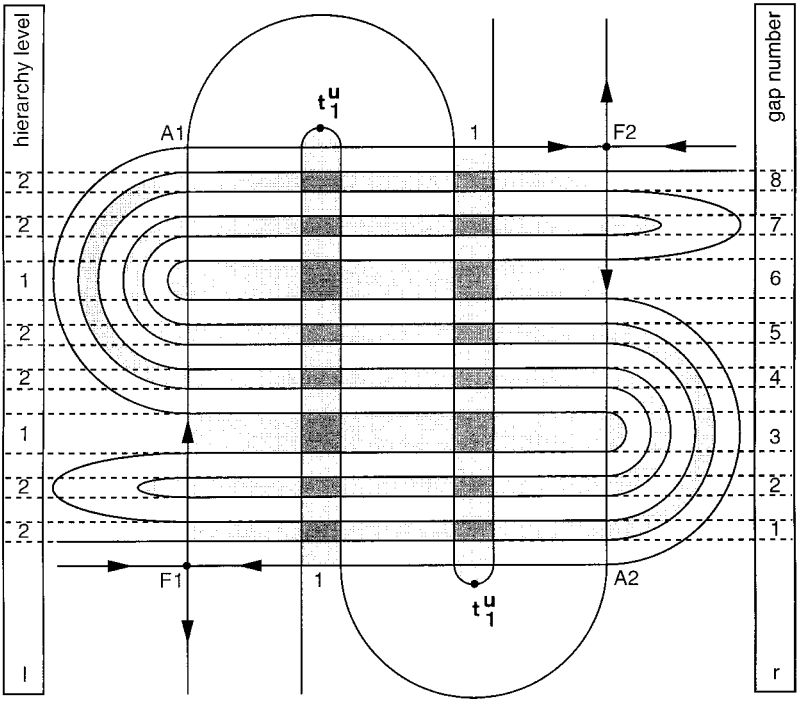

FIG. 3. Schematic plot of a complete ternary symmetric horseshoe. The two outer fixed points are labeled F_1 and F_2. The fundamental rectangle R has the corners F_1, F_2, A_1, A_2. The tendrils of the stable manifolds of F_1 and F_2 are plotted up to level 2, the tendrils of the unstable manifolds are plotted up to level 1. The left column gives the hierarchy number of the gaps cut into R; the numbers in the right column count all gaps up to level 2 consecutively from bottom to top. The formal parameter has the value $\gamma = 1$.

schematically in Fig. 4 is an incomplete ternary horseshoe which belongs to the formal parameter value $\gamma = 4/9$ because t_1^u ends in the fourth gap of order $l \leqslant 2$. Let us emphasize the following prescription for obtaining the correct number r: We must use the gap labels as they hold in the complete case and as they are indicated in the figures in the right-hand-side column. This means that we must also count gaps which are not yet realized by the actual state of the tendrils. Applied to Fig. 4 this rule tells us to include in our counting the gaps with labels 1 through 4 and to obtain $r = 4$ even though the gap with label 2 is not yet formed by the second level tendril of the stable manifold at development stage $\gamma = 4/9$. Compare also the other cases shown.

For nonsymmetric ternary horseshoes we get two parameters γ_1 and γ_2 which can be determined in exactly the same way.

In general for incomplete horseshoes with N elementary fixed points we can have up to $N-1$ formal parameters and their values δ_i are given by

$$\delta_i = r_i N^{-k}. \tag{3}$$

It is important to mention that not all values of formal parameters given by rational numbers of the form of Eq.(3) correspond to cases in which the first stable

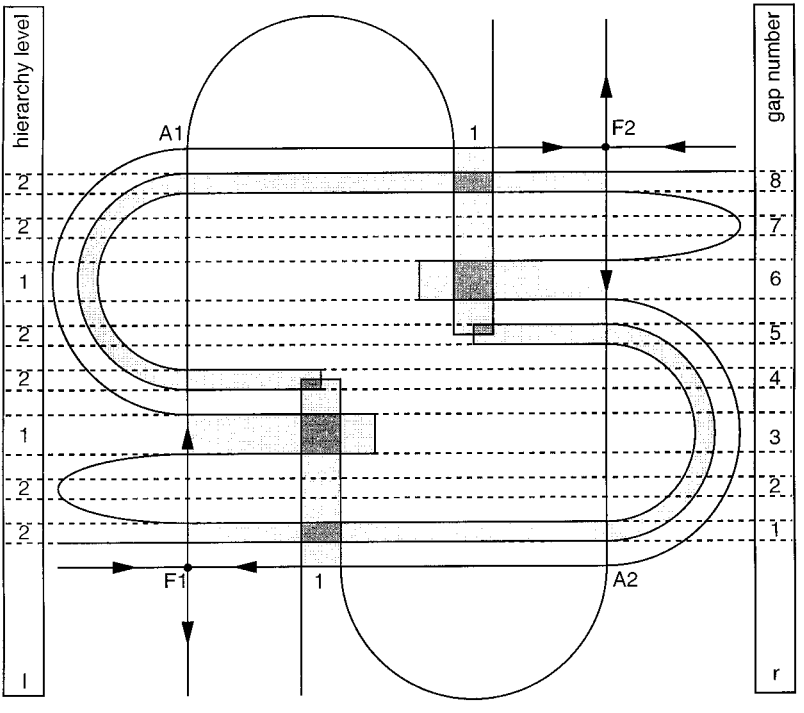

FIG. 4. Schematic plot of an incomplete ternary symmetric horseshoe at formal parameter value $\gamma = 4/9$. The labels are as in Fig. 3.

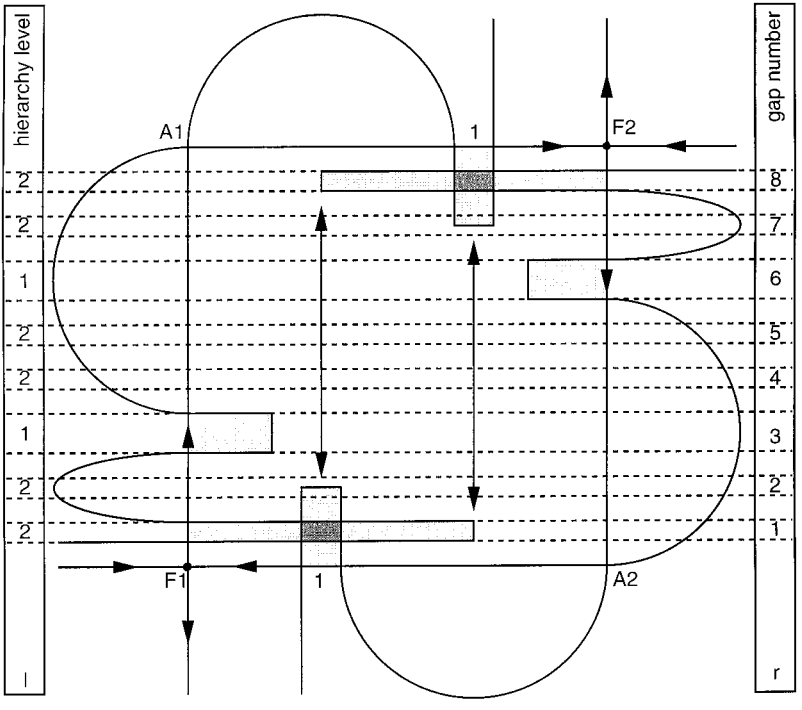

FIG. 5. Schematic view of an incomplete ternary symmetric horseshoe at a development stage $\gamma = 2/9$ where the first level tendril of the unstable manifold does not end in a second-level gap provided by the stable manifolds. Note that the second-level stable tendril does not yet reach far enough to create gap number 2. The labels are as in Fig. 3.

tendril ends in some gap provided by the unstable tendrils. The simplest example for such a case in a binary horseshoe is the value $\beta = 3/8$, where the tendril of level 3 of the stable manifold is too short to build a suitable gap for t_1^u. This case was discussed in more detail in [6]. We get the same situation for a ternary horseshoe at $\gamma = 2/9$. A schematic view of this case is shown in Fig. 5. t_1^u should end in a gap of level 2 of the stable manifold, but the tendrils of the stable manifolds are far too short at this stage of development to provide the necessary gap.

There are many of these non-existing values of the formal parameter. They can be easily sorted out if one considers that in a horseshoe with N elementary fixed points the relative length of the tendrils or, more important, the number of crossings through R grows with a factor N per iteration.

Since the idea of the formal parameter can be understood best by seeing various examples, we recommend that the reader looks up a few additional cases which we have plotted in previous publications: Figs. 2 and 3 in [6] and Fig. 2 in [7] show the binary case $\beta = 1/2$. Figure 10 in [6] shows the binary case $\beta = 1/4$. Figure 3e in [9] shows the ternary symmetric case $\gamma = 1/3$. Figure 1 in [8] shows the ternary

non symmetric case $\gamma_1 = 2/3$, $\gamma_2 = 1$. These references also give the corresponding branching trees and symbolic dynamics.

The classification of a horseshoe by the formal parameter is only partial. It determines rather well the hyperbolic component of the chaotic saddle and neglects the non hyperbolic effects. They are created by the surface of KAM islands and their environment of secondary structures. Accordingly it classifies well the parts of the invariant set which are most important for the scattering behavior. The nonhyperbolic effects only show up in high levels of the hierarchy. In the scattering functions and the branching trees we can recognize them at most in tiny effects visible under extreme resolution. In addition they cause a crossover from exponential to algebraic behavior in the time delay statistics [10–12]. In Section 6 we will discuss whether the observation of nonhyperbolic effects may be of any practical importance for the inverse scattering problem.

The importance and use of the formal parameter mainly stem from the fact that this parameter describes the universal aspects of the growth of horseshoes and ignores the individual aspects. It approximates the development scenario by a description independent of the individual realization of the horseshoe. This becomes clear by considering the fact that the formal parameter indicates the extent to which the tendril of level 1 has already penetrated R. Of course in any development of any horseshoe this relative penetration goes from 0 to 1 during the development of the horseshoe. What actually is unique is the winding numbers of elliptic periodic points and of the KAM islands and thereby the secondary structures around KAM islands and more generally the components of marginal stability. These structures are ignored by our approximate description. However, they are exactly the structures which have little influence on the scattering behavior. In high levels of the hierarchy the invariant manifolds of the outer fixed points penetrate into the surroundings of the KAM islands and their secondary structures. Thus their intersection patterns depend on the fine details of the surfaces of the KAM islands. We do not attempt to include a description or even a classification of these details at high levels.

The important aspect of the horseshoe construction for the inverse scattering problem lies in the following. The invariant set is described by a horseshoe and the structure of the horseshoe is given by the intersection pattern between stable and unstable manifolds of the outer fixed points. The unstable component of the horseshoe is already determined by the pattern in which the various gaps of the stable manifold intersect the local branch of the unstable manifold. As we will see in the following, exactly this intersection pattern can be obtained from scattering measurements. In this sense we can reconstruct the structure of the horseshoe, and therefore the invariant set, from asymptotic measurements. The formal parameter is a compact means for describing the result of this approximate reconstruction.

The main significance of the introduction of the formal parameter and of the restriction to development stages which have a value of the formal parameter whose denominator is small lies in the following: When we change a physical parameter, the tendrils of the manifold become longer or shorter. In general this implies the

occurrence of primary tangencies between stable and unstable manifolds. Accordingly the intersection pattern changes, bifurcations of periodic orbits occur, and the invariant set changes its structure. However, when the tip of the tendril of level 1 ends in a gap which is empty of manifolds, and when accordingly the tips of all higher level tendrils do the same or end outside of R, then small variations and shifts of these tips avoid homoclinic tangencies. This implies a corresponding stability of the structure against bifurcations. Thus we can keep the structure of the invariant set fixed even if we can keep the physical parameter only approximately fixed. Note that the formal parameter remains the same over an entire interval of the physical parameter. The approximation consists in neglecting homoclinic bifurcations done at high levels of the hierarchy when some intersection point splits into three points. This happens frequently also within an interval of the physical parameter which belongs to one value of the formal parameter. These are non-hyperbolic effects which are created in the surrounding of KAM islands.

It is important to mention the relation of the development stage to the value of the topological entropy K_0. For an N-ary horseshoe its value can vary between 0 and $\ln(N)$ during the entire development scenario. For general N-ary horseshoes we can approach completeness along very different routes in the N-1 dimensional parameter space, and general statements about the growth of K_0 along various routes are difficult. Things become simpler for binary or for ternary symmetric horseshoes which only have a single formal parameter. For these cases K_0 is a monotonic function of the formal parameter. Unfortunately we do not have a closed form expression of K_0 as function of β or of γ, but it is easy to obtain this function approximately by a numerical computation for a particular model. For the binary case this numerical plot was given as Fig. 1 in Ref. [6]. For these one parameter cases the value of K_0 yields approximately the development stage of the horseshoe, i.e., the value of the formal parameter. In this way, the knowledge of one of the measures of the chaos provides knowledge of the topological structure of the horseshoe.

3. SCATTERING FUNCTIONS AND THEIR EVALUATION

If the motion in the interaction region can be observed directly, the reconstruction of the horseshoe from this measurement is rather straightforward. In this paper we only consider the situation where the observer does not have direct access to the interaction region and has only the asymptotic preparation of the initial state and the asymptotic measurement of the final state at his disposal.

The first step is to consider the kind of data he can obtain and use as input data for the reconstruction of the internal dynamics. These data are the so-called scattering functions which give properties of the final asymptote as a function of properties of the initial asymptote. The most important example of a scattering function used for the purpose of solving the inverse scattering problem is the time delay function: The observer keeps the initial energy fixed and varies the other initial variables

along a one-dimensional line in the set of all asymptotes. He may scan one asymptotic variable b, e.g., an impact parameter, one relative phase, or an initial momentum, etc., and keep everything else fixed. For each launched trajectory he waits until the system has reached the outgoing asymptotic region, i.e., until some position variable passes a certain value. He monitors the time T; the trajectory needs to reach this stage. Thereby he obtains the function $T(b)$.

This function still has an arbitrariness due to the particular choice of the initial distance r_{in} at which the timing is initiated and the final distance r_{out}, at which the final time T is measured. We can subtract the time the system spends running along the initial and final asymptotes, respectively, from the time T to obtain the time delay ΔT, i.e., the time the system spends in the interaction region.

$$\Delta T(b) = T(b) - r_{\text{in}}/v_{\text{in}} - r_{\text{out}}/v_{\text{out}} \tag{4}$$

where v_{in} and v_{out} are the incoming and outgoing speeds of the projectile, respectively. Later we will mainly be interested in the singularity structure of the scattering functions and for this particular purpose it is irrelevant whether we work with the function $\Delta T(b)$ or simply with $T(b)$. The singular points of both coincide.

The essential property of this function for the sequel is: Whenever the initial asymptote lies on the stable manifold of a localized orbit in the interaction region, then the projectile converges to this localized orbit; i.e., it stays in the interaction region for an infinite time and the time delay function has a singularity. The singularity structure of the scattering function shows how the line of initial conditions pierces the fractal bundle of stable manifolds of the chaotic saddle. Thereby we obtain information about the horseshoe structure and there remains the task of extracting the relevant information from the scattering functions.

For the purpose of illustration we use a time-periodically delta kicked particle in a one-dimensional position space with coordinate q. The momentum of the particle is p and its mass is 1; the period T is also chosen equal to 1. The Hamiltonian function is given by

$$H(p, q) = p^2/2 + V(q) \sum_{n=-\infty}^{+\infty} \delta(t - n - 1/2). \tag{5}$$

To display explicitly the time-reversal invariance of this Hamiltonian system, we choose as times of the stroboscopic map the times between two consecutive kicks. This leads to stable and unstable manifolds that are mirror images of each other under reflection in the q-axis. The map we obtain has the form

$$p_{n+1} = p_n + f(q_n + p_n/2); \qquad q_{n+1} = q_n + p_n + 0.5 f(q_n + p_n/2). \tag{6}$$

The force function f is the negative of the derivative of the potential V. We assume that the force function f falls off rapidly when its argument goes to ∞. The numerical examples shown below correspond to the special choice

$$f(z) = Az(z-1)(z+1)(z^2 + 1/2) \exp(-z^2) \tag{7}$$

of the force function. Here A is a free parameter which acts as the physical parameter of the system. In the asymptotic region this map has the very simple form

$$p_{n+1} = p_n; \qquad q_{n+1} = q_n + p_n. \tag{8}$$

The function f in Eq. (7) has the three zero points $z = -1$, $z = 0$, $z = 1$. This leads to the three fixed points $F_1 = (-1, 0)$, $F_0 = (0, 0)$, $F_2 = (1, 0)$ in the map of Eq. (6). Further fixed points of the map do not exist. In addition it is obvious that the system is invariant under the symmetry $q \to -q$. Therefore the invariant set of the system has the form of a ternary symmetric horseshoe.

Figure 6 presents the time delay function ΔT according to Eq. (4) for the value $A = 6$ of the physical parameter, where the formal parameter of the inside horseshoe construction has the value $\gamma = 1/3$. Here q_{in} is fixed at the value -7 and p_{in} is scanned. To further clarify the meaning of the singularity structure presented by this function we provide in Fig. 7 a look at the stroboscopic plane where the line L_0 shows the line of initial conditions used. The lines L_n are the nth iterates of the initial line. The iterates converge along the stable direction to the boundary of R, are stretched in the unstable direction, and converge toward the local segment of the unstable manifold of the outer fixed point. Of course, intersections of L_0 with the stable manifold are mapped into intersections of L_n with the same stable manifold. Therefore the singularity structure of the scattering function provides us

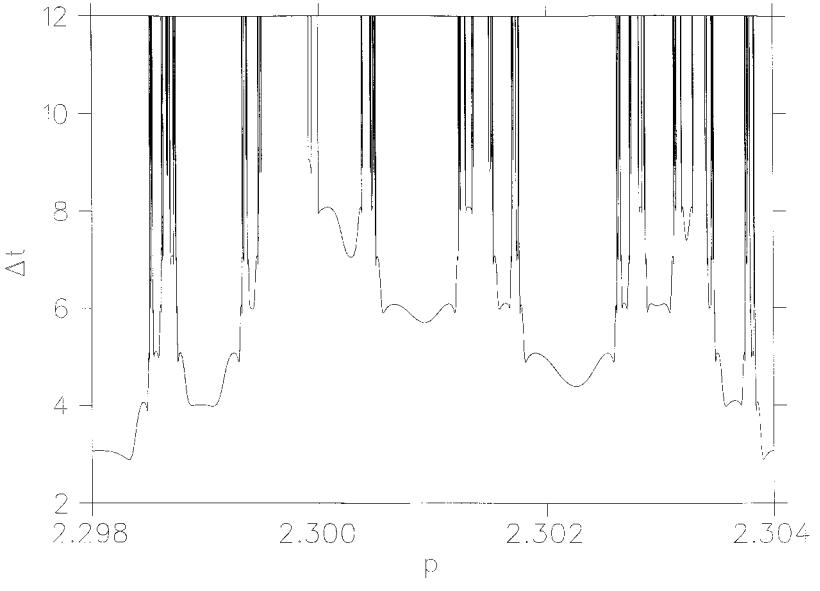

FIG. 6. Time delay function $\Delta T(p_{\text{in}})$ for the system (5)–(7) for the parameter value $A = 6$. q_{in} is fixed at the value -7.

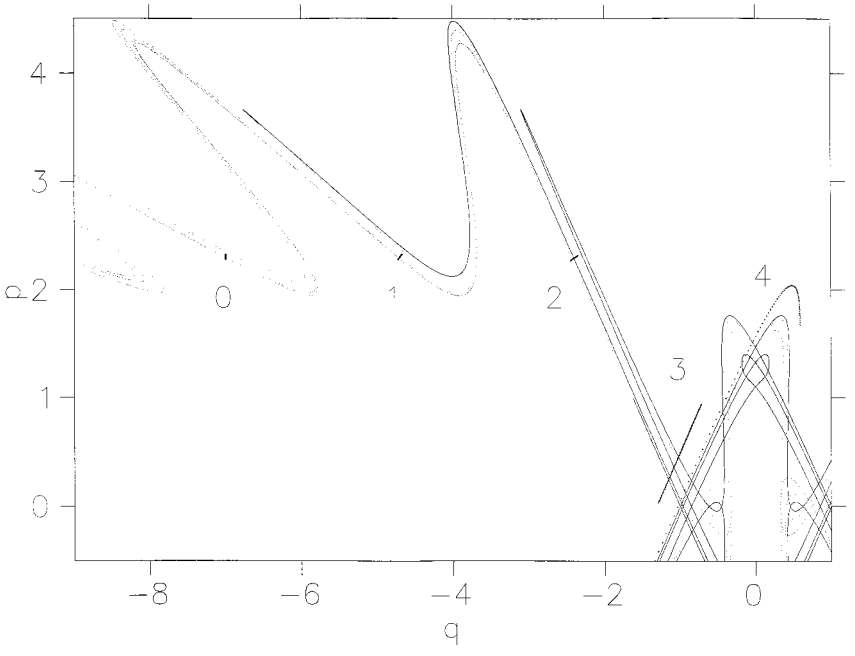

FIG. 7. The horseshoe construction of system (5)–(7) for $A = 6$ in the stroboscopic plane. The formal parameter value is $\gamma = 1/3$. The thin lines are the invariant manifolds of the outer fixed points. The thick line labeled 0 is the line of initial conditions used to obtain the plot of the time delay presented in Fig. 6. The other thick lines are the first four images of the line of initial conditions. They are labeled by the number k of iterations.

with the pattern in which the bundles of stable manifolds intersect the local segment of the unstable manifold. And, most important, the intervals of continuity of the scattering function correspond to the gaps in the bundle of stable manifolds. This pattern coincides with the pattern in which the various tendrils of the stable manifold to the outer fixed points cut gaps into the fundamental rectangle R of the horseshoe construction. According to Section 2 this is all we need to classify the horseshoe.

In this way the information we need in order to reconstruct the topology of the unstable component of the horseshoe is contained in the fractal pattern of singularities and intervals of continuity of the scattering functions. However, one important problem is not yet solved. Viewing the plot of the scattering function, we cannot see directly the level of hierarchy of the various intervals of continuity. But exactly this information is essential to obtain the branching tree. Therefore the next section is devoted to the determination of the levels of hierarchy.

Once we have found the correct hierarchical order of the intervals we can evaluate the information contained in the scattering functions in several ways. First, we obtain the branching tree of the fractal construction. Take a plot of a scattering function, and cut out all intervals of continuity up to level n. In between there remain intervals $I_k^{(n)}$ which contain the so far unresolved regions and which are a

cover of the fractal of singularities. Each of the intervals $I_k^{(n)}$ gives one entry in the branching tree on level n. The entry number k on level n is connected with entry l on level $n-1$, if $I_k^{(n)} \subset I_l^{(n-1)}$.

Second, we can use our knowledge of the correct hierarchical order of the structure of the scattering functions to obtain the quantitative measures of the amount of chaos for the motion in the invariant set by the thermodynamical formalism (for general information about these methods see the textbooks [13–15]; for its application to scattering problems see [16]). To measure the "free energy" we proceed as follows: Measure the length $L_k^{(n)}$ of all the intervals $I_k^{(n)}$; then form the partition sum and fit it to an exponential scaling in n to obtain

$$\sum_k (L_k^{(n)})^\beta \sim \exp(n\beta F(\beta)). \tag{9}$$

Here β is a real parameter which is scanned. For a hyperbolic saddle the sum scales exactly exponentially for sufficiently large values of n and defines the free energy function $F(\beta)$ rigorously. If the saddle is not exactly hyperbolic, then the limit of $n \to \infty$ does not provide exponential behavior but we may find it to good approximation over a significant range of n. For general information about the modification of the scaling properties by nonhyperbolicities see [17, 18]. For practical purposes we can adopt the following strategy: We choose some appropriate intermediate value of n, where the nonhyperbolic effects do not yet take over. Then we obtain measures for the unstable component of the saddle on the corresponding level of hierarchy. An example for such a procedure has been given in [6]. We can determine a function $F(\beta)$ by a comparison of the partition sum for neighboring values of n lying around some central value k and then we can obtain information about the measures which dominate the behavior around the hierarchical level k. For incomplete horseshoes the corresponding values can depend strongly on k and the limit $k \to \infty$ is not well defined. In [6] the following useful numerical observation has been made: If the development stage of the horseshoe corresponds to a value of the formal parameter with a rational value with small denominator and if in addition the physical parameter is close to the lower end of the interval in which the formal parameter has this value, then the nonhyperbolic effects set in at rather high values of the hierarchical level only. And accordingly we obtain a decent scaling behavior of the partition sum over a large range of values of the hierarchical level. From the function $F(\beta)$ we obtain important measures in the following way: Plot the function $\beta F(\beta)$ versus β; its value at $\beta = 1$ is the escape rate of the saddle. This function intersects the β axis in the value of the partial fractal dimension. The value at $\beta = 0$ gives the negative of the topological entropy. Next, we construct the tangent line to this function in the point $\beta = 1$. Its slope is the Lyapunov exponent, it intersects the β axis in the value of the information dimension, and its value at $\beta = 0$ is the negative of the metric entropy. For more details on all these statements see [19, 16]. These measures relate to the Poincaré map rather than to the Hamiltonian flow. A nice explanation of the relation between these measures

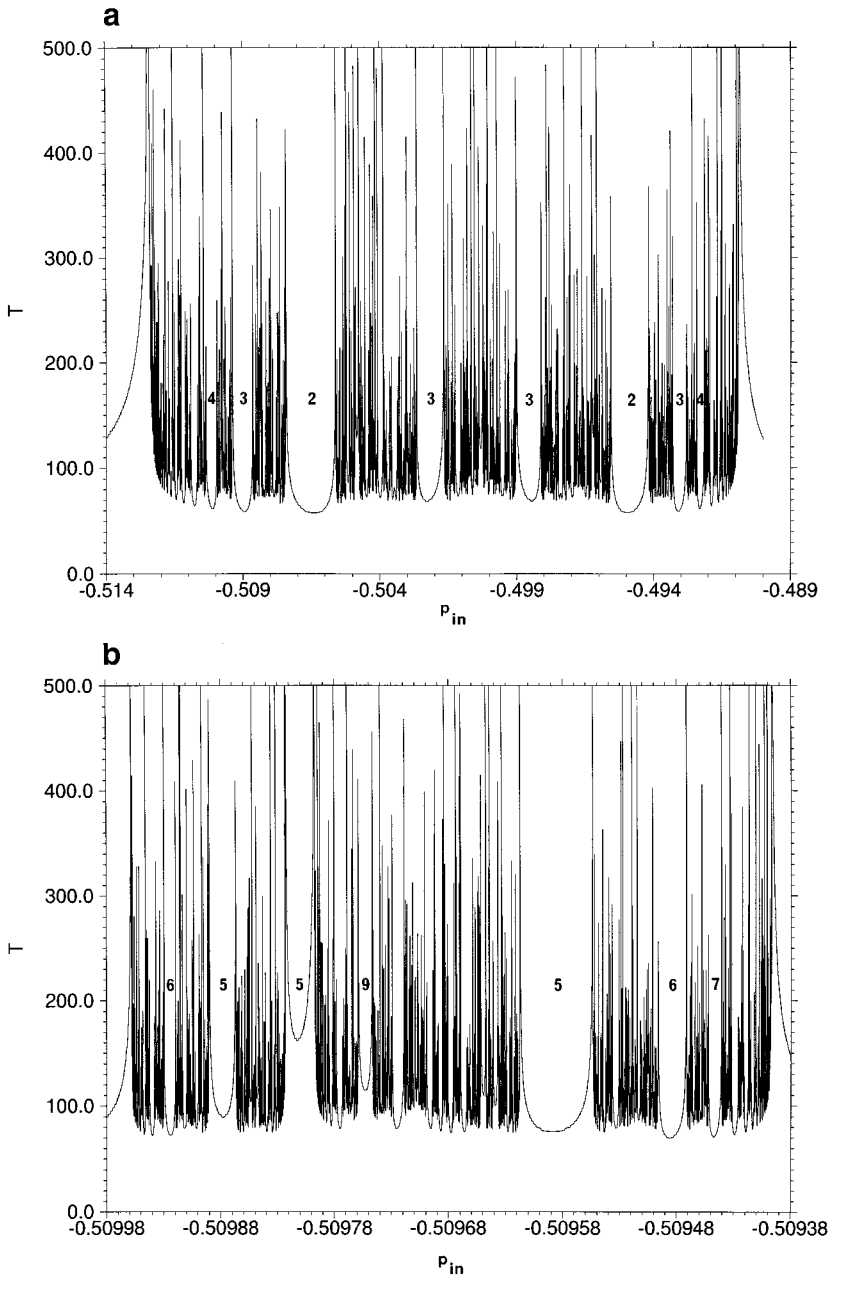

FIG. 8. The function $T(p_{\text{in}})$ for the system defined in Eq. (15) for parameter values $D = 1.5$, $E = -1.11$, $Q_0 = 5.0$. Part (a) shows the function on a domain which covers all singularities. Parts (b, c, d) give magnifications of interesting subintervals. The most prominent intervals of continuity are labeled by their level of hierarchy.

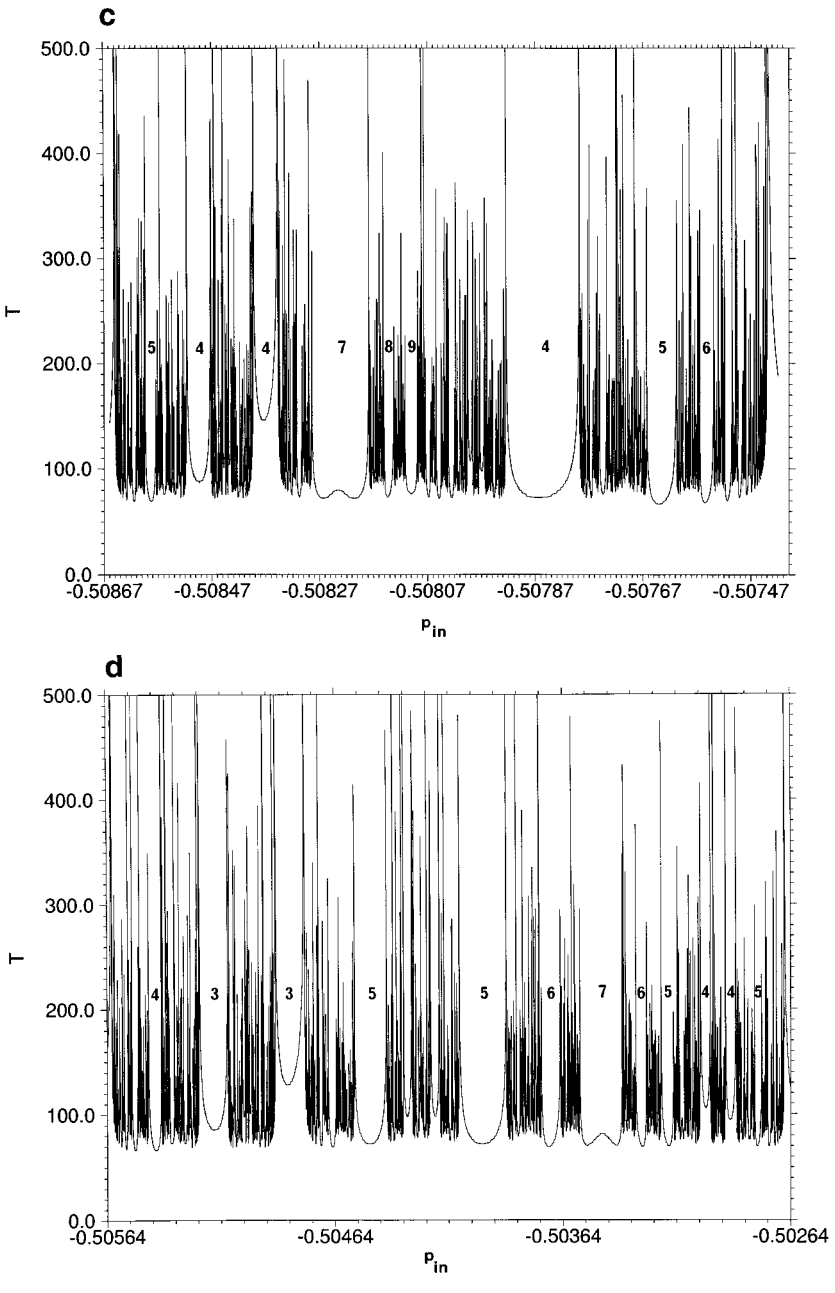

FIG. 8—*Continued*

belonging to the map and the corresponding measures related to the flow in phase space is given in [20].

It is worth emphasizing that so far we have obtained from the information recovered quantitative statements about the saddle, even though we have not yet reconstructed the topological structure and the partition of the horseshoe. However, if we know that we have either a binary horseshoe or a ternary symmetric horseshoe, then knowledge of the topological entropy provides the value of the development parameter approximately, as mentioned at the end of the previous section.

4. RECONSTRUCTION OF THE HIERARCHICAL ORDER

The data which the asymptotic observer obtains are the scattering functions. In the case of a system with topological chaos these functions are singular on a fractal set. As soon as we have found the hierarchical order of this fractal we can recover the branching tree of the horseshoe underlying the chaotic set in the interaction region and we obtain the measures of the chaos. Figure 8 presents as an example the time delay function for a system explained in more detail below. The task is to find the level of hierarchy of the intervals of continuity of this function.

As discussed in [6, 7] the most useful scattering function would be one which gives the number of times a scattering trajectory steps into the fundamental rectangle R of the horseshoe construction. This number is constant in any interval of continuity of the scattering functions and it gives directly the hierarchy level of the interval. In Fig. 8 these numbers are indicated for the largest intervals of continuity. To obtain them directly, an observation of the dynamics inside of the interaction region seems to be necessary. Now we must give a recipe for obtaining the same information from asymptotic measurements only.

A first, naive idea is to look at the minimal values of the time in each interval of continuity, to discretize this number in an appropriate way, and to relate it to the hierarchical level. However, an inspection of Fig. 8 shows immediately that the connection between these two quantities is not monotonic and is by no means obvious. Also, the widths of the intervals of continuity do not show a clear-cut connection to the level of hierarchy.

Next it is shown how, for two classes of scattering system, this problem can be solved by more indirect methods. The first class is systems with a one-dimensional position space and periodic time dependence. They can be reduced to a stroboscopic map, which describes the system completely.

First, the asymptotic observer defines two fundamental regions F_{in} and F_{out} of points in the asymptotic part of the phase space such that every generic scattering trajectory intersects F_{in} exactly once before it enters the interaction region and intersects F_{out} exactly once after it has left the interaction region. Because of the asymptotic form of the map given in Eq. (8) this requirement is fulfilled by choosing the points with a position coordinate q between any convenient q_0 and $q_0 \pm p$,

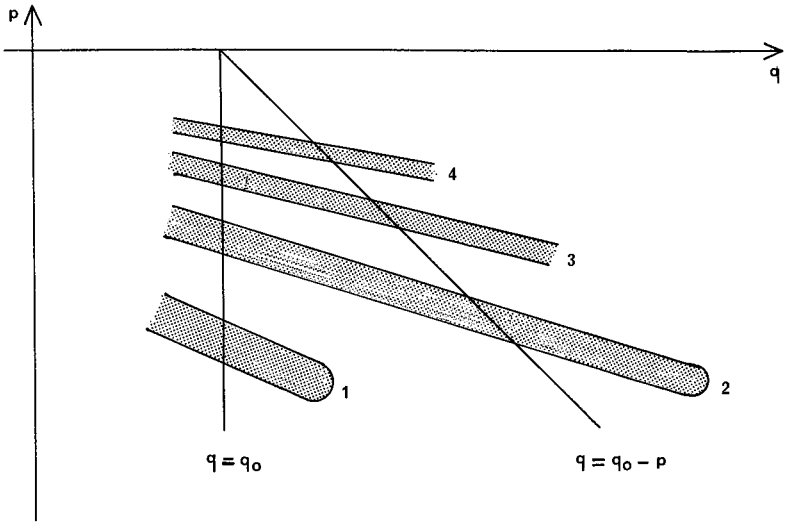

FIG. 9. Schematic plot of the construction of the fundamental wedge in the set of incoming asymptotes. The various tendrils of stable manifolds of the saddle are hatched and are labeled consecutively from bottom to top. For all points lying inside of tendrils (hatched area) this number provides the classification number n referred to in the text. Because of time-reversal invariance and because of the symmetry adapted choice of the plane of section, the corresponding construction in the outgoing asymptotic plane is obtained by a reflection in the q-axis.

where p is the momentum coordinate. Thereby F_{in} and F_{out} are triangular wedges in phase space. The line of initial conditions we use to compute some scattering function can be represented by a line in F_{in}. This construction is visualized in Fig. 9.

Next, we mark the tendrils of the invariant manifolds of the horseshoe in F_{in} and in F_{out}. The asymptotic observer can do this by using asymptotic data only. We scan F_{in} and mark in F_{in} as well as in F_{out} the points which belong to extremely long time delays. In F_{in} and in F_{out} the tendrils create various strips of structures which we label with integer numbers beginning with those with the largest absolute value of p. These consecutive strips belong to consecutive tendrils of the manifold structure. The strip with label $n+1$ belongs to the tendril which is the preimage (if it lies in F_{in}) or the image (if it lies in F_{out}) of the tendril which provides the strip with label n. Figure 9 shows the strips for the example of F_{in}. Because we have chosen a symmetry adapted plane for the stroboscopic map, the corresponding plot for F_{out} is provided by a reflection in the q-axis. We can glue together the two boundary lines of F_{in} to turn the wedge into a cone. The complete set of singularity lines is then a one to one image of a single tendril of the stable manifolds of the horseshoe in the interaction region.

We now proceed to explain the central idea of the reconstruction with the aid of the schematic plot in Fig. 10. In this plot we label the nth tendril of the stable manifolds by T_n^s and the nth tendril of the unstable manifolds by T_n^u. The nth gap

cut into R by the stable and unstable manifolds is labeled by G_n^s and G_n^u, respectively. Let us pick an initial point p_0 lying in some gap inside of the tendril of the stable manifolds. For easier display in the plot we assume it lies in tendril T_3^s; in reality it should lie in the intersection of the wedge F_{in} with some T_n^s. We have also assumed that the gap which contains p_0 has hierarchical level 2. Now we study the trajectory of p_0 under iterated application of the map M. The nth image of p_0 is called p_n.

By the horseshoe construction it is clear that the image of any point of T_n^s lies in T_{n-1}^s and the image of any point in T_k^u lies in T_{k+1}^u. Therefore the point p_2 lies in T_1^s. For our further argumentation it is essential that the image of T_1^s be G_1^u. Therefore all points of T_1^s which do not belong to the small hatched area in Fig. 10 are mapped into R. The hatched area may be considered to be a gap of level 0 in the stable manifolds. Trajectories belonging to points in this area will never enter R. The image of the hatched part of T_1^s is the hatched part of G_1^u. In the following we only consider trajectories starting in parts of T_n^s which do not belong to the iterated preimage of the hatched area. From the considerations presented so far it is clear that points belonging to T_n^s but not to these preimages will be mapped into the intersection between G_1^u and R under n applications of the map.

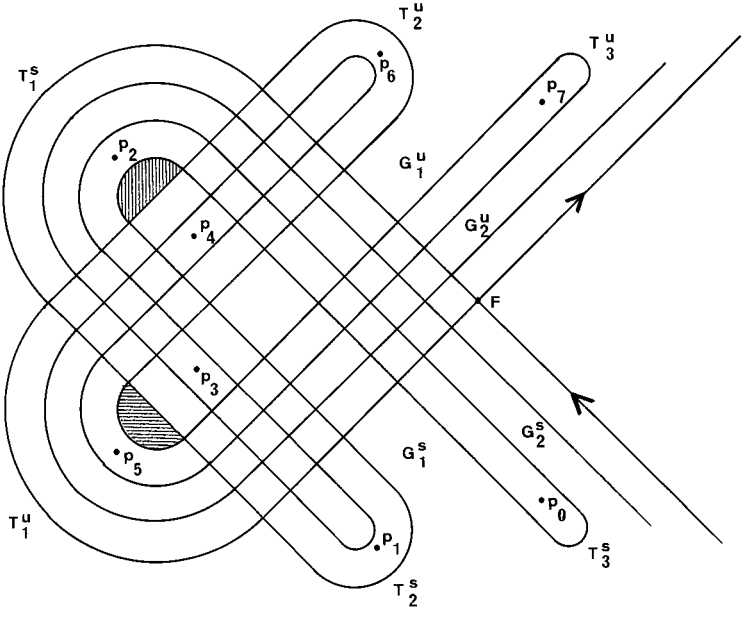

FIG. 10. Schematic plot of a horseshoe to demonstrate how we obtain the number of times a trajectory steps into the fundamental rectangle R from the asymptotic properties of this trajectory. In the tendril T_1^s the small area A, which is not mapped into R, is hatched. The image of A is the hatched tip of G_1^u which lies outside of R. One trajectory is plotted which steps into R twice, p_{n+1} is the image point of p_n under the map. It is assumed that the initial point p_0 lies in a gap of level 2 of the tendrils of the stable manifold.

Next, we need to know the number of steps of the map the trajectory will stay inside of R, i.e., how many times we must apply the map M in order to map the point lying in G_1^u to a point outside of R. We may proceed as follows: M maps G_m^s into G_{m-1}^s as long as m is larger than 1. The image of G_1^s is just T_1^u. Therefore, to any point lying in the intersection of R and G_m^s we must apply M exactly m times in order to map the point into T_1^u and thereby to map it outside of R for the first time. The same holds true for any point lying in the intersection of G_1^u with G_m^s. For the example trajectory included in the plot of Fig. 10 the point p_3 belongs to the intersection between G_1^u and G_2^s. Accordingly this trajectory has two points inside of R, namely p_3 and p_4.

The following observation is essential to the sequel: If the first point of the trajectory of point p_0 which enters R belongs to the intersection between G_1^u and G_m^s, then the trajectory has m points inside of R and the gap in which p_0 lies will obtain the hierarchical level m. The empty gaps in T_n^s and therefore the intervals of continuity of the scattering functions are the preimages of the gaps, which the various G_m^s cut into G_1^u. By determining the hierarchy of the gaps we obtain this intersection pattern, which is equivalent to the branching tree.

We now know that point p_{n+m} lies in T_1^u. Then $k-1$ further applications of M are necessary before the point $p_{n+m+k-1}$ of the trajectory can be observed in the outgoing asymptotic region as a point appearing in the intersection of T_k^u with F_{out}. We have come to the following result: An initial point p_0 is chosen in the intersection of F_{in} with T_n^s at time $t_{\text{in}}=0$ and at the later time $t_{\text{out}}=j\cdot T$ the trajectory is observed in the intersection between F_{out} and T_k^u. The trajectory needed a total of j applications of the map to come from the initial point p_0 to the observed final point. It needed n steps to enter R and it needed $k-1$ steps after it left R. Therefore this trajectory has $m=j-n-k+1$ points lying inside of R and the gap of T_n^s to which p_0 belongs, i.e. the interval of continuity of the scattering functions to which p_0 belongs, has hierarchical level m. In the example trajectory in Fig. 10 these numbers are $n=3$, $j=7$, $k=3$, from which we obtain the correct value $m=2$.

Unfortunately we do not know the levels of the tendrils which belong to the various segments of tendrils seen inside of F_{in} and F_{out}. In the construction explained above and in Fig. 9 we have labeled these segments observed in F_{in} and F_{out} consecutively starting from some arbitrary number for the segment with the highest absolute value of the momentum. But we do not know the number of tendrils completely missing in F_{in} and F_{out}. The first tendrils are too short to ever reach these asymptotic wedges. However, we can be sure that the difference between the true level of the tendril and the number we have assigned in F_{in} and F_{out} is the same integer number for all tendrils. Therefore their order stays intact. By using the labels in F_{in} and F_{out} instead of the correct levels of the tendrils we make the same unknown error for all trajectories and we can obtain at least the correct difference in the hierarchical levels for all gaps. Fortunately, this is sufficient for a correct reconstruction of the branching tree.

With the aid of these observations the recipe for determining how the hierarchy number (up to a global constant) is provided by asymptotic observations becomes

clear: Start some trajectory in a gap of strip number n in F_{in}. After some number j of steps of the map, i.e. after time $t = j \cdot T$, the trajectory appears in F_{out}, say in strip number k. Then we know that it needed $n + l$ steps to enter R and $k + l - 1$ steps after it left R, where we do not know the correction number l, the difference between the true level of any tendril and the number we have assigned to it in F_{in} or F_{out}. From these numbers we know that the trajectory has stayed for a number $m = j - n - l - k - l + 1$ of steps inside of R. We are only able to get the number $z = m + 2 \cdot l = j - n - k + 1$. The number z is the hierarchy number we assign to the gap, in which the trajectory has started. By applying this procedure to a representative trajectory in any gap, we obtain the hierarchical order of the entire structure of gaps in the tendrils, up to the same global constant $2 \cdot l$. The difference between the numbers of any two gaps gives the correct difference of their hierarchical label. In these differences the global constant drops out and they are all we really need to obtain the correct branching tree.

Applying this method to the time delay function shown in Fig. 6 we obtain the corresponding hierarchy function shown in Fig. 11. The function value assigns to each initial value the hierarchical level of the interval of continuity of the delay function, to which this point belongs. Also indicated in this figure is a possible symbolic code for the intervals $I_k^{(n)}$ which cover the fractal on level n. The corre-

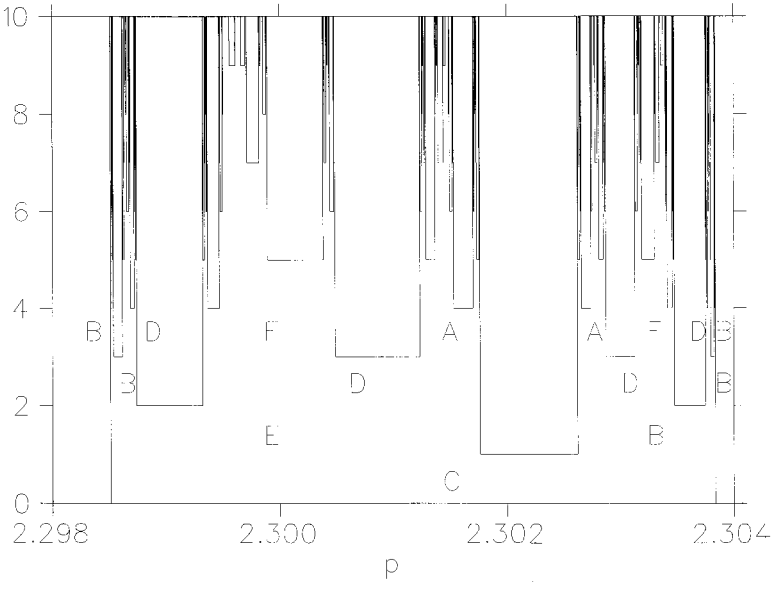

FIG. 11. Result of the construction of the hierarchy function for the system defined in Eqs. (5)–(7). The parameters are the same as those used for Fig. 6. This plot is to be compared with Fig. 6. A comparison of the two functions assigns to each interval of continuity of the function in Fig. 6 as hierarchy level the corresponding value of the function plotted here. In addition, this figure contains for the four lowest levels a symbolic code for the intervals $I_k^{(n)}$ which cover the fractal on level n.

sponding branching tree coincides with the one we expect for a ternary symmetric horseshoe of development stage $\gamma = 1/3$. A direct numerical construction of the horseshoe (see Fig. 7) confirms this suggestion.

It is clear that the method presented here does not depend on a particular example and transfers directly to any time periodic scattering system on a one-dimensional position space.

We show how this method still can be applied to particular time-independent systems in two dimensions provided they have what we may call an internal clock and provided that this clock is at least approximately decoupled from the external motion. Thus this internal clock can be used in analogy to the external clock from the previous example. This, e.g., is the case for a certain class of three particle systems with rearrangements on a one-dimensional position space. As an example we use a variant of the Calogero–Moser system [21]. The particles are labeled A, B, C; their position coordinates are q_A, q_B, q_C and their canonical momenta p_A, p_B, p_C. All three masses are set to the value 1. The Hamiltonian is given by

$$H = (p_A^2 + p_B^2 + p_C^2)/2 - D_A(\cosh(q_B - q_C))^{-2} - D_C(\cosh(q_A - q_B))^{-2} + D_B(\sinh(q_C - q_A))^{-2}. \tag{10}$$

We consider the symmetrical case $D_A = D_C = D$ only, and without loss of generality we set $D_B = 1$. If the total energy is $-D < E < 0$, then there are two open arrangement channels: In channel A the particle A is isolated and far away from the bound state formed by particles B and C. In channel C the particle C is isolated and far away from the bound state formed by particles A and B. First, the center of mass motion can be separated. In the mass weighted relative coordinates

$$Q = \sqrt{2/3}q_B - q_A/\sqrt{6} - q_C/\sqrt{6} \tag{11}$$

$$y = (q_C - q_A)/\sqrt{2} \tag{12}$$

and the corresponding canonical momenta

$$P = \sqrt{3/8}(p_B - p_A - p_C) \tag{13}$$

$$w = (p_C - p_A)/\sqrt{2} \tag{14}$$

the following Hamiltonian with two degrees of freedom remains

$$H = (P^2 + w^2)/2 - D_A(\cosh(\sqrt{3/2}Q - y/\sqrt{2}))^{-2} - D_C(\cosh(\sqrt{3/2}Q + y/\sqrt{2}))^{-2} + D_B(\sinh(\sqrt{2}y))^{-2} \tag{15}$$

For each value of Q we denote by $y_m(Q)$ the value of $y > 0$ for which the potential of Eq. (15) has its minimum along the line $Q = \text{constant}$. We can visualize this as the bottom of the potential valley. This curve together with the condition $w > 0$ will define the surface of section S for the Poincaré map M. In S we use the coordinates

Q and p_t. The latter is the component of the momentum tangential to the line of intersection. The distance along this intersection line, i.e., along the valley, is the reaction coordinate and thus p_t is the momentum belonging to the reaction coordinate. The coordinates Q and p_t are not a canonically conjugate pair; nevertheless they are convenient and useful coordinates in S. For symmetry reasons there is always a fixed point at $Q=0$, $p_t=0$. It corresponds to the trajectory oscillating on the line $Q=0$. For $D<1$ there are no further localized trajectories in the phase space and no further periodic points in S. For $D>1$ there is a ternary symmetric horseshoe in S. The point $Q=0$, $p_t=0$ is its central fixed point. The two outer fixed points are at $Q=\pm\infty$, $p_t=0$.

The asymptotic observer next wants to identify the branching tree of this horseshoe and if he knows the basic type (in our case ternary symmetric) he can thereby also find the value of the development parameter γ. Let us assume he sits at a point Q_0 in the asymptotic region and prepares the systems in the Poincaré plane at $Q_{\text{in}}=Q_0$ with momenta $p_t=p_{\text{in}}$. The other coordinates are fixed by the intersection condition and by the total energy E. The observer starts the trajectory at time $t_{\text{in}}=0$ and checks the time t_{out} at which the system comes out of the interaction region again hitting the Poincaré plane S at some $Q_{\text{out}}>Q_0$ or some $Q_{\text{out}}<-Q_0$ for the first time with $p_t=p_{\text{out}}$. In the former case the final asymptote belongs to arrangement A, in the latter case it belongs to arrangement C. Figure 8 shows the example of t^{out} as a function of p_{in} for $E=-1.11$ and $Q_0=5.0$ for parameter value $D=1.5$. The task of the observer is to reconstruct the hierarchical order in the intervals of continuity of this function.

The fact that the outer fixed points of the horseshoe are at infinite distance implies that the observer must be inside these fixed points. By restricting the observation to sufficiently large values of p_t the observation is still outside the fundamental rectangle and can be considered asymptotic. We shall see later that indeed the larger values of p_t are those that are appropriate for our purposes. To avoid the problem of fixed points at infinity we could include small potential wells in the potential valley at some $Q=\pm Q_1$ such that the depth of the potential valley decreases for $|Q|>Q_1$. Then the outer fixed points are shifted near Q_1 and when we choose $Q_0>Q_1$ the observer sits outside of R.

As a first step the asymptotic observer makes a plot of all occurring combinations of values of t_{out} and p_{out} while he fixes $Q_{\text{in}}=Q_0$ and $t_{\text{in}}=0$ and scans p_{in}. The result is shown in Fig. 12. At least in parts of the plot a discretization of the time values is obvious. This shows that the system has some internal clock and that it is sufficiently well decoupled from the external motion to be useful for our purpose. The clock motion is the transversal oscillation in the potential valley. Figure 12 shows that the clock is kept in phase for short times at all values of p_{out} while for very long times only smaller values of this momentum fulfill the condition. The values near zero for p_{out}, which we may not consider according to the above argument, are reached only for very long times that are probably always impractical. To find the hierarchical level of any interval of continuity it is sufficient to evaluate a single trajectory from this interval. And, in general, initial conditions picked from

the middle of the interval correspond to points in Fig. 12 lying in the well ordered region. The points in the upper right part of the plot correspond to trajectories spending a long time in the interaction region performing complicated motion there. Thereby they have their internal clock dephased. The label of the strip is the number (up to an unknown global constant) of oscillations which the system has made in the transverse direction in the potential valley between the initial preparation and the final detection. By construction of our Poincaré section condition it is also the number of times the trajectory has crossed the section line in positive orientation and thereby it is the number of applications of the map we need in order to map the initial point taken from F_{in} into the final point detected in F_{out}. This number plays the role which the number j played in the previous example.

In addition the asymptotic observer can plot into the Poincaré plane the points corresponding to trajectories which have spent a long time in the interaction region. The result is shown in Fig. 13. The structures are the tendrils of the unstable manifolds of localized trajectories. Again the observer can cut out a triangular region F_{out}, which is a fundamental region in the sense that every outgoing asymptote into arrangement A intersects this region once. To put the asymptotes into arrangement C he can do a corresponding plot at large negative values of Q. The use of this plot is exactly the same as that in the previous example of systems

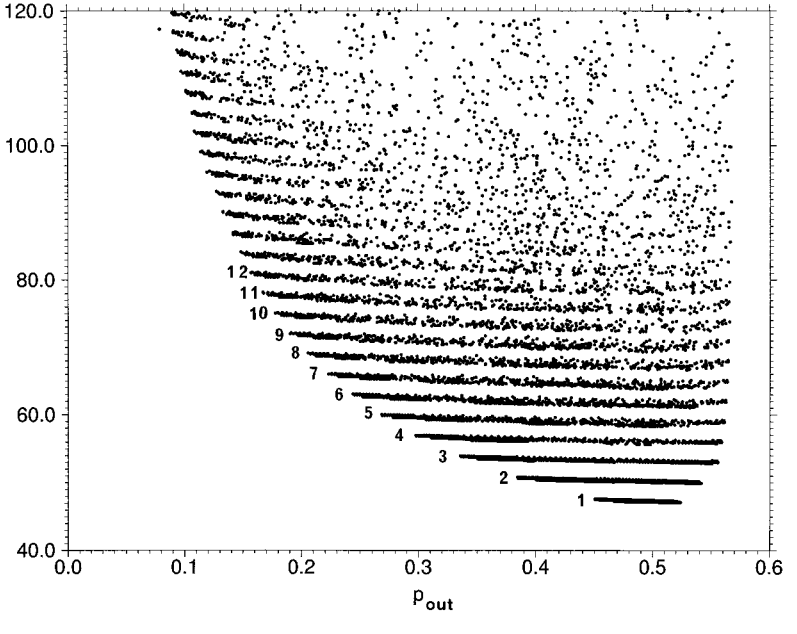

FIG. 12. A plot of the occurring combinations of values of p_{out} and t_{out} for the system of Eq. (15) at parameter values $D = 1.5$, $E = -1.11$, $Q_0 = 5.0$, used in Fig. 8. The various strips are labeled consecutively from bottom to top. This number provides the classification number j needed in Eq. (16) for the points lying in the corresponding strip.

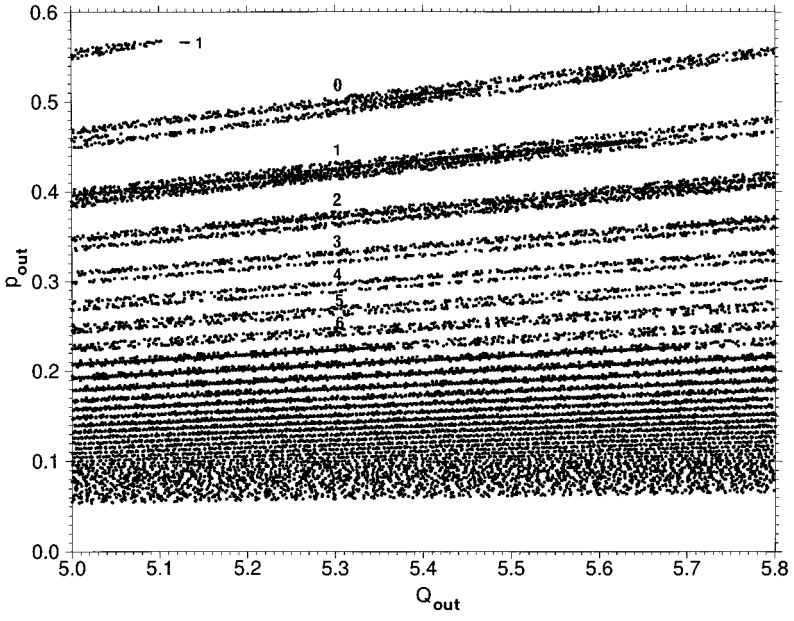

FIG. 13. Plot of the unstable manifolds of the saddle in the plane of outgoing asymptotes for system (15) at parameter values used in Figs. 8 and 11. The tendrils are labeled consecutively from top to bottom. This number provides the classification number k needed in Eq. (16) for the points lying in the corresponding strips.

with periodic dependence on time. That is, the two numbers we obtain, one for the initial asymptote and one for the final asymptote, are the levels (again up to a global constant) of the tendrils of the stable and unstable manifolds, respectively, in which the initial point has been prepared and the final point has been detected, respectively. They play the same roles as the numbers n and k of the previous example.

The procedure for finding the hierarchical level of any interval of continuity of the time function of Fig. 8 is now clear. We pick a particular trajectory from each interval of continuity in one of the tendril strips of F_{in}, measure the time it needs to come back into the fundamental region F_{out}, and record the values of $Q = Q_{\text{out}}$, $p_t = p_{\text{out}}$, and t_{out} with which it reaches the region F_{out}. This provides points in the plots of Figs. 12 and 13, respectively. If the initial point was chosen well, the final point lies in the region of Fig. 12, which is ordered into well separated strips. This assigns a mapping number j to the trajectory. The strip into which it falls in Fig. 13 gives the number k that we must subtract. The difference $m = j - k$ gives uniquely the hierarchy number m of the interval up to a global constant n_0, which is the same for every trajectory taken from the same strip of tendrils in F_{in}. If we pick initial points from different strips in F_{in}, we must, in addition, subtract the corresponding strip number to which the initial point belongs. This is in analogy

to the subtraction of n in the previous example. Let us take, for example, the trajectory with initial points $Q = 5.0$, $p_t = -0.5064$ (see Fig. 8). The outgoing point has the values $Q_{\text{out}} = 5.5398...$, $p_{\text{out}} = 0.5237...$, $t_{\text{out}} = 47.1228...$. From the plots of Figs. 12 and 13 we read off $j = 1$, $k = 0$.

In this special example we may even determine the value of n_0, though it is not necessary for our purpose. In Fig. 8 we have $n_0 = 1$ because the line of initial conditions misses the gap of level 1. If this guess were be wrong, it would not cause any problem because the differences between level numbers are the only important information. According to this guess we have for all intervals

$$m = j - k + 1 \tag{16}$$

With this formula we compute the level number of all intervals above a certain width and find the numbers written in Fig. 8. The resulting branching tree is exactly that of the ternary symmetric horseshoe at $\gamma = 2/3$. A direct construction of the Poincaré map in the interaction region confirms this result.

In both examples presented we have used in an essential way the existence of an external (in the first example) or internal (in the second example) clock of the system which the asymptotic observer can see. In addition the intersection condition which defines the surface of section for the Poincaré map is coupled to this clock; the intersection condition is the passing of a particular phase of the oscillatory motion of the clock. Thereby the observer can read off the total number of steps of the map which map the prepared initial point into the detected final point. Similar methods are not applicable to systems without clocks, such as the scattering of a point particle off a local short range potential. Thus completely different ideas for the determination of the hierarchical level of the intervals of continuity of scattering functions are needed. So far we do not have a general method which works for all systems. However, inspection of the Fig. 8 provides the following vague suggestion: On the boundary points of each interval of continuity sit singularities, and they produce flanks reaching into the interval. These flanks from both sides fill up the interval partially and are the reason why the bottom of the interval does not have the value n in appropriate units, where n is the hierarchical level. Instead the value can be considerably higher in some cases. There seems to be a rough measure of the strength of this flank effect: It is approximately proportional to the distance up to the next interval of equal or smaller level of hierarchy. In this way we could find the true depth of the bottom value of the interval (hierarchical level) by consistently subtracting values proportional to the distance to the next interval of equal or smaller level. Unfortunately so far we have not brought this idea into a practical form that works for arbitrary systems.

5. COINCIDENCE OF DEVELOPMENT SCENARIOS

So far the asymptotic observer has obtained the exact branching tree and thereby has obtained the necessary input data for an evaluation of the measures of the

chaotic set by the thermodynamical method. When he wants to go a step further and reconstruct the topological structure of the horseshoe from scattering data, the following interesting problem emerges: A discrete uncertainty occurs which cannot be resolved by knowledge of the scattering functions only. The question is, Which basic kind of horseshoe do we encounter? For example, is it a binary or a ternary symmetric horseshoe, or something more complicated? The source of the confusion is that several different basic types of horseshoes can lead to the same branching tree over many levels of hierarchy [22], if we choose appropriate values of the formal parameter and, therefore, corresponding values of the physical parameter. Even worse, all the development scenarios look the same, as we vary the physical parameter. From the equality of the branching tree it becomes evident that knowledge of, e.g., the topological entropy is of no help in answering this question. In this section we explain this problem in detail for the simplest case, namely for the distinction between a binary and a ternary symmetric horseshoe.

To illustrate the problem let us look at the branching tree of a ternary symmetric horseshoe at formal parameter $\gamma = 1/3$. This horseshoe was presented in Section 3 (see Fig. 7) and its branching tree can be seen in Fig. 11. It is a binary branching tree up to level 9. Starting from level 9, deviations from the binary structure emerge. The first deviation can be seen at around $p_{\text{in}} = 2.996$. However, when we measure with limited resolution and have the branching tree only up to some finite level (in this particular example only up to level 8), the branching tree could be misinterpreted as that of a complete binary horseshoe. The question remains whether there are methods for resolving discrete uncertainties of this type.

A first idea might be to change the physical parameter and see from the change of the branching tree in which situation we are. Unfortunately this method does not work. The reason is that all the development scenarios coincide in such a way that to each binary horseshoe there is a corresponding ternary symmetric horseshoe with the same branching tree up to levels of the hierarchy where nonhyperbolic effects set in [22]. More precisely: The formal parameter of a binary horseshoe can be written in the form

$$\beta = \sum_{i=0}^{k} a_i/2^i, \tag{17}$$

where the sum runs over a finite number of i values. To make the representation unique, we require that a_i take only the values -1 or 0 or $+1$ and in addition we require that $a_{i+1} = 0$ when $a_i \neq 0$. In the same way we represent the possible values for the formal parameter of the ternary horseshoe in the form

$$\gamma = \sum_{i=0}^{k} a_i/3^{i+1} \tag{18}$$

with the same restrictions for the values of a_i. Equal sequences of a_i lead to corresponding branching trees for the hyperbolic component of the invariant set. And the

TABLE I

Corresponding values of the Formal Parameters β and γ for Binary and Ternary Symmetric Horseshoes up to Hierarchical Level $i=5$ and Coefficients a_i in the Developments of Eqs. (17), and (18).

β	a_0	a_1	a_2	a_3	a_4	a_5	γ
1/32	0	0	0	0	0	1	1/729
1/16	0	0	0	0	1	0	1/243
1/8	0	0	0	1	0	0	1/81
1/4	0	0	1	0	0	0	1/27
9/32	0	0	1	0	0	1	28/729
7/16	0	1	0	0	−1	0	26/243
15/32	0	1	0	0	0	−1	80/729
1/2	0	1	0	0	0	0	1/9
17/32	0	1	0	0	0	1	82/729
9/16	0	1	0	0	1	0	28/243
5/8	0	1	0	1	0	0	10/81
21/32	0	1	0	1	0	1	91/729
11/16	1	0	−1	0	−1	0	71/243
23/32	1	0	−1	0	0	−1	215/729
3/4	1	0	−1	0	0	0	8/27
25/32	1	0	−1	0	0	1	217/729
13/16	1	0	−1	0	1	0	73/243
27/32	1	0	0	−1	0	−1	233/729
7/8	1	0	0	−1	0	0	26/81
29/32	1	0	0	−1	0	1	235/729
15/16	1	0	0	0	−1	0	80/243
31/32	1	0	0	0	0	−1	242/729
1	1	0	0	0	0	0	1/3

Note. The two-parameter values of β and γ in the same line lead to a binary and a ternary symmetric horseshoe with the same branching tree.

order of the corresponding cases is preserved. Table I gives a compilation of the corresponding formal parameter values for binary and symmetric ternary horseshoes up to level 5. It also includes the common sequence of values of a_i.

To distinguish the scenarios of a binary and a symmetric ternary horseshoe one might vary the parameter to large values and check whether the entropy never grows beyond ln(2). Unfortunately, one faces the following problem: There are systems in which the horseshoe first grows along the binary scenario until it has reached the complete binary stage, where it remains for a finite interval of the physical parameter. However, under further increase of the physical parameter the horseshoe continues to evolve beyond the complete binary case. Such a behavior can be created by two different mechanisms: First, the tendrils of the horseshoe can bend back. The tips of tendrils which lie outside of R in the binary complete case penetrate from outside into R. This case is realized by the scattering of a charged particle off a magnetic dipole [7]. Second, inside of R, saddle-center bifurcations

can occur, which insert additional small, incomplete horseshoes into the previously complete case. An example of this type has been studied in [23]. It is the scattering of a particle from a rotating hard disc. For any integer k there exists an open interval of the physical parameter (the Jacobi constant J in this special case), where a complete horseshoe with k fixed points is realized. Such an example demonstrates the following: If we observe a scenario in which the topological entropy grows beyond $\ln(N)$, this does not exclude the possibility that for some interval of the physical parameter the development scenario will run along that for a horseshoe with k elementary fixed points, where k can be any integer with $k \leqslant N$. These counterexamples show that no systematic method for determining a horseshoe's basic type can be based on observations of branching trees and their change under changes of the physical parameter only.

Furthermore, a saddle-center bifurcation of fixed points or a pitchfork bifurcation of an elementary fixed point may also occur in the incomplete case. Thereby an incomplete horseshoe may jump from one development scenario into a different one, where the number of elementary fixed points differs by two.

On the other hand we may obtain relevant information from the observation of symmetries. Such observations, for example, can distinguish between the binary and ternary symmetric cases for a time dependent system on a one-dimensional position space. We shoot in particles from one side and scan a line of initial conditions. In the case of the binary horseshoe all particles come out on the same side. In the ternary case particles beginning in some intervals of continuity of the scattering function leave on one side. Those starting in other intervals of continuity leave on the other side. Furthermore, in the case of a symmetric ternary horseshoe the behavior is symmetric when we shoot in from the other side. From these symmetry properties we can conclude that we have a symmetric horseshoe with an odd number of elementary fixed points. The same idea works for the symmetry between the arrangement channels A and C in the Calogero–Moser system. However, these symmetry considerations cannot distinguish a ternary horseshoe from an incomplete one with five fixed points, where the central fixed point of the ternary one is replaced by a tiny ternary horseshoe. This might occur, if the central fixed point of a ternary horseshoe suffers a pitchfork bifurcation and splits into three fixed points. The effects of this bifurcation might be on such a tiny scale that the asymptotic observer with limited resolution does not recognize the bifurcation and is convinced that he continues to observe a ternary horseshoe.

Interesting connections between an exactly binary branching tree, a rather complicated invariant set, and symmetry occur in one of the standard paradigms of chaotic scattering given by the system of three hard discs. If they are sufficiently far apart this system is strictly hyperbolic [24, 25]. It is an instructive example for the nonuniqueness of the step from the branching tree to the horseshoe. This system has five fundamental periodic orbits, three bouncing orbits between pairs of discs, and two cyclic orbits with opposite orientation touching the three discs in turn. The branching tree is exactly binary, because no disc can be touched twice without touching another disc first. So after each collision the decision is binary as to which

of the two other discs is touched. Therefore the first guess of the asymptotic observer may be that he has found a system governed by a complete binary horseshoe. As can be deduced from the set of fundamental periodic orbits, the invariant set has a more complicated structure. Symmetry can be used to explain the apparent connection to a binary horseshoe and to project the actual invariant set on a binary one. In the symmetric case, where the centers of three equal discs are located at the corners of an equilateral triangle, the $\mathscr{C}_{3v}$ symmetry allows one to reduce the five fundamental orbits to only two by appropriate identification. This leads to the well-known complete binary horseshoe. This reduction to a binary system persists for sufficiently small deviations from the $\mathscr{C}_{3v}$ symmetry due to structural stability of hyperbolic systems. We discuss these issues more extensively in the Appendix, where we show that the construction of an adequate surface of section leads to an invariant set with 12 basic periodic points, the identification of which becomes nontrivial if we deviate from the symmetric case. Note that in this example "sufficiently small" actually may allow for quite large asymmetries as we retain a complete (and thus hyperbolic) horseshoe as long as one disc does not block trajectories connecting the other two, because this would cause pruning.

In general, knowledge of the topological structure of the horseshoe was not necessary for finding the correct hierarchical order of the branching tree and thus for constructing a symbolic dynamics. However, this knowledge is essential for constructing the partition of phase space. Once we have the structure of the horseshoe we can apply the standard method to the construction of a partition. In the partition the division lines run along the primary folds of the horseshoe construction [26, 27]. Some problems associated with this method have been observed [28, 29], but the method has been improved to eliminate inconsistencies [30, 31]. In a new version even KAM tori can be included in the partition scheme and in the resulting symbolic dynamics. However, to achieve this, it is necessary to know the winding numbers of the central periodic points in the KAM tori. This is an information which cannot be obtained from the scattering data since the interior of KAM tori cannot be reached by scattering trajectories. Thereby the best we can get from scattering data is some reconstruction of the globally unstable component of the invariant set. Accordingly only a partition and a symbolic dynamics of this component are relevant for comparison with scattering data. The connection between the truncation of the horseshoe and pruning of the symbolic dynamics is established by construction of a well ordered symbolic plane in which truncation of the horseshoe is indicated by the monotonic advance of a pruning front. Thus all the symbolic blocks reached by the pruning front are forbidden [32]. For successful applications of these ideas to various bound systems see [33–37].

However, from the point of view of the inverse scattering problem this standard method has a disadvantage. The number of partition regions and therefore the number of symbols for the symbolic dynamics is equal to the number of basic fixed points of the horseshoe. For the symbolic dynamics of the branching tree derived from the scattering functions we like to use in many cases a number of symbols larger than the number of basic fixed points of the underlying horseshoe. Therefore

in general the symbolic dynamics derived for the horseshoe by the standard method is different from the symbolic dynamics constructed for the branching tree. The reason is that the standard method introduces boundary lines of the partition regions which partially are not given by tendrils of the invariant manifolds of the outer fixed points. To obtain the corresponding symbolic dynamics in the branching tree we would have to introduce in the branching tree corresponding artificial divisions of intervals of continuity. This seems unnatural from the point of view of the inverse scattering problem. This problem is not a main concern of this paper but will be explained in more detail in [38].

As an example of a symbolic dynamics constructed simply from knowledge of the branching tree of a scattering function we have included in the low level entries in Fig. 11 a possible symbolic dynamics in six symbolic values. This seems natural from the point of view of the inverse scattering problem, and it is able to accommodate the symmetry of the system and the fact that the branching tree is created by a ternary symmetric horseshoe. The rules are: After A or F either A or C follows, after B or E follows either B or D follows, after C either B or E, follows, and after D either A or F follows. Of course, this labeling is to a large extent arbitrary; there are many other possibilities. These rules are exactly binary, and therefore they break down at places in the branching tree where nonhyperbolic effects, i.e., nonbinary branchings appear.

6. FINITE RESOLUTION AND NONHYPERBOLIC EFFECTS

Nonhyperbolic effects typically occur at high levels of the hierarchy. Finite resolution of observation may thus become a problem, which we address in this section.

The procedure of the observer may be as follows: He has physical parameters at his disposal and obtains branching trees, let us say up to level $n+2$. Let us assume that he knows that the underlying horseshoe is binary. Thereby he can decide whether the formal parameter is below, inside, or above any allowed value of the form $k/2^m$ for the formal parameter, where $m \leqslant n$. For any practical purposes it is advisable to set the physical parameters well inside such intervals of the formal parameters. This guarantees that the formal parameter will not change with small variations of the physical parameters, which an experimentalist can never control with infinite precision. In this sense the true value of the introduction of the formal parameter is that, even with limited control of the physical parameters, we can fix the formal parameter exactly.

By fixing some value of the formal parameter the structure of the saddle is not determined completely. Only some universal properties of the development scenario are determined, since each horseshoe must pass through the entire sequence of formal values while it develops from some initial stage at parameter value zero toward completeness. Beyond the universal scenario each individual realization of the horseshoe at the corresponding development stage can show individual properties

starting at some level of the hierarchy above the hierarchical level m of the formal parameter stage. The usual situation is that, at the lower end of the formal parameter interval, the individual properties and therefore also the possible nonhyperbolic effects set in at rather high levels of the hierarchy only. As we increase the physical parameter to approach the upper end of the interval in which the formal parameter stays constant, the individual properties and nonhyperbolic effects reach lower levels. Note that the formal parameter for a given N-ary horseshoe may be restricted to a smaller interval if bifurcations create or annihilate elementary fixed points as the physical parameter is varied. Our considerations must then be restricted to intervals between two consecutive events of this type.

Some of the values of the formal parameter, especially those near completeness, allow for exactly hyperbolic incomplete horseshoes. The completely hyperbolic case $\beta = 7/8$ for the binary horseshoe has been represented in [39]. For a few more examples see [40, and 8]. Which of the possible hyperbolic situations are realized in a particular system is not known a priori. The existence of incomplete hyperbolic cases requires, in particular, sufficiently large eigenvalues of the basic fixed points. If hyperbolic situations are realized then generally several different ones exist for the same value of the formal parameter. They differ in grammatical rules at high levels. The hyperbolic situation closest to the boundary toward lower values of the parameter usually has the shortest and simplest grammatical rules of its symbolic dynamics. In general the hyperbolic situations, belonging to some value of the formal parameter, do not fill the corresponding interval of the physical parameter completely.

Unfortunately, this additional complication prevents the systematic use of hyperbolic situations for the classification of horseshoes from asymptotic data. For example, one might think that a binary horseshoe at parameter $\alpha = 7/8$ could be distinguished from a ternary horseshoe at parameter $\gamma = 26/81$ by the fact that the ternary horseshoe can never be exactly hyperbolic, in contrast to the binary horseshoe, which frequently is exactly hyperbolic. However, there are two different objections. First, the binary horseshoe might be a rare case, where the eigenvalues of the fixed points are in such an unfavorable ratio that the hyperbolic situations inside the $\alpha = 7/8$ interval are not realized. Second, in the ternary case the onset of nonhyperbolic effects can be at such a high level of the hierarchy that we cannot recognize it with the limited resolution at our disposal. The same holds for the distinction of the ternary case $\gamma = 1/3$ from the binary case $\beta = 1$.

The second point is attenuated by the fact that we can detect nonhyperbolicity from the power law in the long time tails of the time delay statistics, where we expect a behavior like $t^{-3/2}$ when KAM islands influence the scattering process, and t^{-2} when parabolic surfaces influence the process but KAM islands do not. Such tails can often be detected with less resolution than that necessary to reconstruct the bifurcation tree. In some cases (e.g., Rydberg molecules where Coulomb interactions are important) the time delay may be strongly distorted and statistics may have tails that are neither exponential nor $t^{-3/2}$ nor t^{-2}. Thus time delay statistics does not seem helpful.

7. CONCLUSIONS

The reconstruction of properties of the chaotic saddle from asymptotic data was the aim of our inverse scattering analysis. The procedure can be decomposed into several steps:

The first step is the extraction of the branching tree from a scattering function such as the time delay function. The problem is basically to determine the level of hierarchy to which a given interval of continuity corresponds. We were able to give a satisfactory solution of this problem for two important classes of systems, namely one-dimensional systems with a periodic time dependence and two-dimensional systems with a *built in clock*, *i.e.*, a fixed or nearly fixed internal frequency. This implies that the internal clock is at least approximately decoupled from the external motion, which is typically the case if one degree of freedom is bound and either will not be excited or is excited in an isochronous form. Isochronous behavior is typical of harmonic systems, which often are a good approximation of small excitations. The observer should choose a surface of section for the Poincaré map, which is coupled to this clock in such a way that the intersection condition is associated with some particular phase of this clock. The observation of this clock enables the asymptotic observer to know the total number of steps of the Poincaré map which the system needed to map the prepared initial point into the measured final point. To this end it is advisable for the observer to prepare the system in the plane of section and also to measure in this plane.

Knowledge of the branching tree allows for construction of a symbolic dynamics and for evaluation of thermodynamic quantities. If we have independent information on the basic structure of the horseshoe we may deduce its degree of development and its formal parameter. Here the numerical value of the topological entropy obtained by the thermodynamical method is certainly of great help. If the underlying horseshoe is binary or ternary symmetric, its value alone determines the formal parameter and thereby the development stage of the horseshoe to good approximation.

This leads us to the second step of our analysis. Unfortunately the basic type of the horseshoe, i.e., the number of basic fixed points, cannot be read off from the branching tree alone. For different basic types, at least at the lower levels of hierarchy, not only the branching trees themselves, but even the development scenarios as a function of the physical parameter, are equal over a wide range of the formal parameter. If we knew all levels of the hierarchy and happened to find each hyperbolicity at some value of the formal parameter we could resolve this question. But to consider infinite amounts of discrete information is unrealistic even in the absence of errors. At the moment we do not know how to obtain the additional information we need from scattering functions alone. The basic type of the horseshoe must to be found by some other methods, e.g., by symmetry considerations. Some symmetries can actually be detected by asymptotic measurements. These will work for simple horseshoes, but will certainly find their limitations in complicated cases. In other cases we may have the information on grounds that go beyond scattering analysis.

The typical case of incomplete horseshoes is not hyperbolic. The branchings and infinite grammar involved with the fractal thicket surrounding the integrable islands are usually not of interest and we have not even attempted to obtain this information from scattering data. Rather, we limited our discussion to pointing out that this situation may often be detected by the long power law tails of the time delays, even when it is not obvious from the value of the formal parameter.

We finally pass to the discussion of the inverse problem with errors in the data. In this case we certainly need an exactitude that allows us to reconstruct the branching tree to a sufficiently high level of hierarchy. The problem of identifying the basic type of the horseshoe becomes even more difficult and will lead to discrete ambiguities typical of inverse problems with error.

Summarizing, we may say that for certain classes of problems we have shown how the bifurcation tree can be reconstructed from asymptotics, and the formal parameter can be determined if, e.g., symmetry considerations allow us to fix the basic type of the horseshoe. The formal parameter in turn gives an approximate characterization of the unstable component of the invariant set.

APPENDIX

The scattering of a point particle from three hard discs is a paradigm that has been investigated frequently since Refs. [24, 25] were published. All the results of the hard discs hold true in an analogous way for the scattering from three soft potential mountains as described in [41]. For simplicity we shall describe mainly the system with hard discs. Assume that the radius of the discs is sufficiently small compared to the distance between their centers that the branching tree of the scattering functions is binary complete [24, 25]. This implies exact hyperbolicity of the invariant set. Essentially this condition requires the absence of geometrical screening of some trajectories. The horseshoe of the three-disc system becomes incomplete if the discs come too close compared to their radius such that some localized trajectories disappear. In the case of soft potential mountains this effect sets in if the energy reaches the height of the potential saddles from above. When the completeness condition is fulfilled for the case with $\mathscr{C}_{3v}$ symmetry, where the centers of the three discs of equal radii sit on the corners of an equilateral triangle, then it remains fulfilled for sufficiently small deviations from this symmetry because of the structural stability of an exactly hyperbolic case.

Let us label the three discs A, B, C. There are five different elementary periodic orbits, which are needed for overshadowing the arbitrary trajectories of the invariant set. There are three different trajectories, which in the following we call the bouncing orbits, that always bounce between the same two discs. Let us call b_A the orbit which bounces between discs B and C, b_B the orbit which bounces between discs C and A, and b_C the orbit which bounces between discs A and B. There are two different ring-shaped orbits; one's orientation is the reverse of the

other's. Let us call a_+ the orbit which touches the discs in the sequence A, B, C, etc., and a_- the one which touches the three discs in the order A, C, B, etc.

When we introduce a surface of section S it is desirable to choose it such that it fulfills the following two requirements: First, all localized trajectories, i.e., all trajectories belonging to the invariant set, must intersect the surface. Second, at least in the neighborhood of all trajectories belonging to the invariant set, the surface must be transversal to the flow. It is easy to check, by elementary geometrical considerations, that we can never use the crossing of a single straight line in position space to define a surface fulfilling these conditions. Therefore it is appropriate to choose a surface that has several disconnected components, with each component defined as the crossing of a straight line in position space. For their choice the following observation is important. Whenever the geometry of the discs is such that the branching tree is exactly binary, then in the center between the three discs there is a region which is never entered by trajectories of the invariant set. Therefore we can choose three half-lines in position space which start in this central region, each runs into a different gap between two discs, and they must extend beyond the bouncing orbit. We take each of these three lines in duplicate to have both orientations. This provides six lines of intersection and six corresponding pieces of a two dimensional plane in the energy surface which will be used as surface of section to construct a Poincaré map. In the symmetric case we choose the lines that are symmetry related, the three half-lines are transformed into each other by the rotations of $\pm 2\pi/3$, the orientations are reversed, and two of the three half-lines are exchanged by each of the three reflections of $\mathscr{C}_{3v}$. We call the surface generated by the intersection line σ_C which runs between the discs A and B and has positive orientation S_{C+}, etc. The

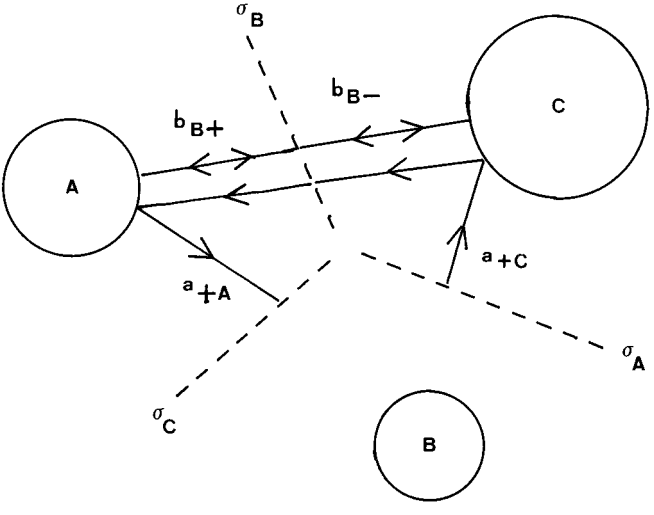

FIG. 14. Plot of the choice of intersection lines in the three-disc system. Also shown are four elementary orbit segments. For an explanation of the notation see the text.

complete surface of section S is the union of the six components. Figure 14 gives a schematic plot of the geometrical situation.

Each of the bouncing orbits is cut into two segments by these intersection lines. For example, the orbit b_A is cut into one half, which we label b_{A+}; it runs from the intersection line σ_A to the disc C, then back to the intersection line σ_A and into the other half, b_{A-}. Similar rules hold for the decomposition of the other bouncing orbits by interchanging indices. In a natural way the ring orbit a_+ is cut by the intersection lines into three segments; the one segment labeled a_{+A} starts from σ_B, hits the disc A, and ends in the intersection line σ_C. Analogous notations are created for the other segments by an exchange of labels, and for the ring orbit with negative orientation, by switching to the $-$ labels. Thereby we obtain 12 different elementary orbit segments, which we use for the overshadowing process in the following scheme: Let us assume a trajectory has scattered from disc C, moves toward disc A, and is back scattered such that next it will hit disc C again. Then the segment from the crossing of line σ_B up to the next crossing of line σ_B is structurally the same as orbit segment b_{B+} and will be overshadowed by it. In the next case assume the trajectory has scattered from disc C, moves toward disc A, and is scattered here such that it will next hit disc B. Thus the segment from the crossing of line σ_B up to the crossing of line σ_C is structurally the same as orbit segment a_{+A} and will be overshadowed by it. Similar considerations hold for the other segments.

Now it becomes clear why the branching tree is exactly binary. First, because of the convexity of the discs it is clear that the projectile can never hit the same disc twice without hitting any other disc in between. Whenever a trajectory approaches some disc, it has the binary choice which of the two other discs to hit next. Accordingly, of the 12 elementary segments which can be used for the overshadowing process there is the choice between 2 different segments which can be attached to continue the trajectory smoothly in every crossing of an intersection line. General scattering trajectories have a finite number of hits with discs and accordingly must to make a finite number of binary decisions about how to continue the trajectory. This leads to topological entropy $\ln(2)$ of the system and to an increase like $c \cdot 2^n$ of the number of scattering trajectories with n bounces that have different overshadowing sequences. Finally, this leads to the exactly binary structure of the branching tree extracted from scattering functions.

From the complicated structure of S with its six connected components it is clear that the invariant set is not represented by the usual type of binary horseshoe with two elementary fixed points in S. Rather, the elementary points are three different orbits of the map of period 2 (belonging to the bouncing orbits) and two different orbits of the map of period 3 (belonging to the ring orbits). In each connected component of the surface of section there lie exactly one point stemming from a bouncing orbit and one point stemming from a ring orbit. In each of the six components of S we have a structure equivalent to a binary horseshoe, but the mapping connects the various components.

We come to the usual binary horseshoe construction by identifications according to the $\mathscr{C}_{3v}$ symmetry. We identify all six components of S, all six segments of

bouncing orbits, and all six segments of ring orbits among themselves. Then the two remaining points in S representing the bouncing orbit and the ring orbit, respectively, become fixed points of the map in S. Overshadowing of the orbits is done by two elementary segments and the corresponding symbolic dynamics describes the sequence of bouncing trajectory and ring trajectory segments as they come in sequence. The symmetry properties of the trajectories and of the Poincaré map for the case of three soft potential mountains have been reported in detail in [42].

In an experiment we can observe the $\mathscr{C}_{3v}$ symmetry without difficulty. We perform a sequence of measurements of the scattering functions in which we keep the incoming energy fixed and vary the incoming direction as well as the incoming impact parameter. The observer notices the $\mathscr{C}_{3v}$ symmetry in each scattering function, and of course also in the branching trees seen from symmetry related choices of the lines of initial conditions.

Because the complete binary case is hyperbolic and therefore structurally stable, at least topologically the structure imposed by the $\mathscr{C}_{3v}$ symmetry remains intact under sufficiently small symmetry breaking deformations. The identification of the structures in the six components of S requires an appropriate smooth coordinate transformation in each of them. Formally we can recover the $\mathscr{C}_{3v}$ symmetry by the following mechanism: First, we construct a smooth point transformation that transforms the deformed problem into the original symmetric one. This transformation can be extended to phase space to form a canonical transformation C, and due to the structural stability mentioned above there must exist at least one choice for this transformation that does not change the character of the horseshoe on S. We can now define a different but isomorphic symmetry group $\mathscr{C}_{3v}$ with elements $C^{-1}gC$, where $g \in \mathscr{C}_{3v}$. In such a way a horseshoe of the usual complete binary type might be recovered also in the "nonsymmetric" case. The exactly binary structure of the branching tree leads to the usual complete binary horseshoe only by this symmetry reduction. It does not display this standard form without the identification and does not show it in a naive choice of the surface of section.

ACKNOWLEDGMENTS

C. Jung thanks CONACyT for a beca patrimonial. This work was supported by the UNAM DGAPA Project IN-102597.

REFERENCES

1. J. B. Keller, I. Kay, and J. Shmoys, *Phys. Rev.* **102** (1956), 557.
2. R. G. Newton, "Scattering Theory of Waves and Particles," 2nd ed., Springer-Verlag, Berlin/New York, 1982.
3. C. Jung and T. H. Seligman, *Phys. Rep.* **285** (1997), 77.
4. S. Smale, *Bull. Am. Math. Soc.* **73** (1967), 747.
5. E. Ott, "Chaos in Dynamical Systems," Cambridge Univ. Press, Cambridge, UK, 1993.

6. B. Rückerl and C. Jung, *J. Phys. A* **27** (1994), 55.
7. B. Rückerl and C. Jung, *J. Phys. A* **27** (1994), 6741.
8. W. Breymann and C. Jung, *Europhys. Lett.* **25** (1994), 509.
9. C. Lipp and C. Jung, *J. Phys. A* **28** (1995), 6887.
10. C. F. Karney, *Physica D* **8** (1983), 360.
11. B. Chirikov and D. L. Shepelyansky, *Physica D* **13** (1984), 395.
12. C. F. Hillermeyer, R. Blümel, and U. Smilansky, *Phys. Rev. A* **45** (1992), 3486.
13. D. Ruelle, "Thermodynamic Formalism," Vol. 5 of "Encyclopedia of Mathematics and Its Applications," Addison–Wesley, Reading, 1978.
14. C. Beck and F. Schlögel, "Thermodynamics of Chaotic Systems," Cambridge Univ. Press, Cambridge, UK, 1993.
15. R. Badii and A. Politi, "Complexity: Hierarchical Structures and Scaling in Physics," Cambridge Univ. Press, Cambridge, UK, 1997.
16. T. Tel, *in* "Directions in Chaos" (H. Bai-lin, Ed.), Vol. 3, p. 149, World Scientific, Singapore, 1990.
17. P. Grassberger, R. Badii, and A. Politi, *J. Statist. Phys.* **51** (1988), 135.
18. A. Politi, R. Badii, and P. Grassberger, *J. Phys. A* **21** (1988), L763.
19. T. Tel, *J. Phys. A* **22** (1989), L691.
20. R. Badii, *Chaos* **7** (1997), 694.
21. F. Calogero, *in* "Nonlinear Phenomena" (K. Wolf, Ed.), Springer-Verlag, Berlin, 1983.
22. C. Lipp, C. Jung, and T. H. Seligman, *in* "Proceedings, IV Wigner Conference," (N. M. Atakishiyev, T. H. Seligman, and K. B. Wolf, Eds.), p. 180, World Scientific, Singapore 1996.
23. N. Meyer, L. Benet, C. Lipp, D. Trautmann, C. Jung, and T. H. Seligman, *J. Phys. A* **28** (1995), 2529.
24. B. Eckhardt, *J. Phys. A* **20** (1987), 5971.
25. P. Gaspard and S. Rice, *J. Chem. Phys.* **90** (1989), 2225.
26. P. Grassberger and H. Kantz, *Phys. Lett. A* **113** (1985), 235.
27. P. Grassberger, H. Kantz, and U. Moenig, *J. Phys. A* **22** (1989), 5217.
28. F. Giovannini and A. Politi, *Phys. Lett. A* **161** (1992), 332.
29. K. T. Hansen, *Phys. Lett. A* **165** (1992), 100.
30. F. Christiansen and A. Politi, *Phys. Rev. E* **51** (1995), R3811.
31. F. Christiansen and A. Politi, *Nonlinearity* **9** (1996), 1623.
32. P. Cvitanovic, G. H. Gunaratne, and I. Procaccia, *Phys. Rev. A* **38** (1988), 1503.
33. K. T. Hansen, *Nonlinearity* **6** (1993), 753.
34. K. T. Hansen, *Phys. Rev. E* **51** (1995), 1838.
35. G. Tanner, K. T. Hansen, and J. Main, *Nonlinearity* **9** (1996), 329.
36. A. Bäcker and H. R. Dullin, *J. Phys. A* **30** (1997), 1991.
37. K. T. Hansen and S. Güttler, *J. Phys. A* **30** (1997), 3421.
38. C. Lipp and C. Jung, *Chaos*, in press.
39. M. J. Davis, R. S. MacKay, and A. Sannami, *Physica D* **52** (1991), 171.
40. G. Troll, *Chaos* **3** (1993), 459.
41. C. Jung and H. J. Scholz, *J. Phys. A* **20** (1987), 3607.
42. C. Jung and P. H. Richter, *J. Phys. A* **23** (1990), 2847.